AJRCCM Articles in Press. Published on 04-June-2018 as 10.1164/rccm.201711-2300OC

A Disintegrin and A Metalloproteinase-9 (ADAM9): A Novel Proteinase Culprit with Multifarious Contributions to COPD

Xiaoyun Wang, PhD[†]

Francesca Polverino, MD, PhD[†‡]

Joselyn Rojas-Quintero, MD, MSc[†]

Duo Zhang, PhD[§]

José Sánchez, PhD[¶]

Ilyas Yambayev, MD[†]

Eva Lindqvist, MSc[&]

Robert Virtala, MSc[&&]

Ratko Djukanovic, MD[*]

Donna E. Davies, PhD[*]

Susan Wilson, PhD[**]

Rory O'Donnell, PhD[£]

Danen Cunoosamy, PhD[&&]

Petra Hazon, PhD[&&]

Andrew Higham, PhD [††]

Dave Singh, MD[††]

Henric Olsson, PhD[&&]

Caroline A. Owen, MD, PhD[†‡]

[†]Division of Pulmonary and Critical Care Medicine, Brigham & Women's Hospital, Harvard Medical School, Boston, MA 02115, USA; [‡]The Lovelace Respiratory Research Institute, Albuquerque, NM 87108, USA; [§]Pulmonary Center, Boston University School of Medicine, Boston, MA, 02118, USA; [¶]Quantitative Biology, Discovery Sciences, AstraZeneca R&D, Gothenburg,

Molndal, Sweden; [&]Study Enterprise, Early Clinical Development IMED, AstraZeneca R&D Gothenburg, Molndal, Sweden; [&&]Bioscience Lung Epithelium, Respiratory, Inflammation & Autoimmunity IMED, AstraZeneca R&D, Gothenburg, Molndal, Sweden; [*]NIHR Southampton Respiratory Biomedical Research Centre and Clinical and Experimental Sciences, Faculty of Medicine, University of Southampton, Southampton, UK; [**]Histochemistry Research Unit, Faculty of Medicine, University of Southampton, Southampton, UK; [£]St. James's Hospital, Dublin, Ireland; [††]Medicines Evaluation Unit, University of Manchester, Manchester University NHS Foundation Trust, Manchester, UK.

Address for correspondence: Caroline A. Owen, MD, PhD; Division of Pulmonary and Critical Care Medicine, Brigham and Women's Hospital, 60 Fenwood Road, 3rd Floor, Room 3016H, Boston, MA 02115. Phone: 617-525-5408; Fax: 617-525-5413; Email: cowen@bwh.harvard.edu

Author contributions: CO conceived the project and designed the experiments; XW, FP, JR, DZ, JS IY, RD, DD, SW, RO, JS, AH, DS, RV, EL, JS, HO, and CO conducted experiments and contributed to data analysis and interpretation. All authors contributed to the writing and editing of the manuscript.

Source of support: This work was supported by Public Health Service, National Heart, Lung, and Blood Institute Grants HL063137, HL086814, HL111835, PO1 HL105339, P01 HL114501, and NIAID grant #AI111475-01, Flight Attendants Medical Research Institute grants #CIA123046 and YFEL141004, Parker B. Francis Foundation Fellowship, the Brigham and Women's Hospital-Lovelace Respiratory Research Institute Consortium, and The Department of Defense (CDMRP) grant # PR152060.

Running Title: ADAM9 in the Pathogenesis of COPD

Descriptor Number: 9.13

Word count for the body of the manuscript: 3599

AJRCCM Articles in Press. Published on 04-June-2018 as 10.1164/rccm.201711-2300OC

At a glance commentary

Scientific knowledge on the subject:

Matrix metalloproteinases have been strongly implicated in the pathogenesis of emphysema, but less is known about the contributions of proteinases to other key COPD phenotypes including small airway fibrosis and mucus hyper-secretion. The contributions of proteinases with a disintegrin and a metalloproteinase domain (ADAMs) to the pathogenesis of COPD have not been explored.

What this study adds to the field:

ADAM9 staining is increased in lung epithelial cells and macrophages in smoker lungs, and even more so in COPD lungs, and correlates directly with pack-year smoking history and inversely with airflow obstruction and FEV_1 % predicted. *ADAM9* gene expression is increased in bronchial brushing cells from COPD patients versus controls and correlates directly with pack-year smoking history. In mice exposed to cigarette smoke, Adam9 promotes the development of several key COPD-like phenotypes (emphysema, small airway fibrosis, and mucus cell metaplasia). Adam9 promotes emphysema development by increasing lung inflammation and inducing alveolar septal cell apoptosis by shedding growth factor receptors from cell surfaces. Thus, ADAM9 is a multifarious culprit in COPD that could be targeted therapeutically to limit disease progression and ameliorate symptoms associated with several COPD phenotypes.

This article has an online data supplement, which is accessible from this issue's table of content online at www.atsjournals.org

Abstract

Introduction: Proteinases with **a d**isintegrin and **a m**etalloproteinase domain (ADAMs) have not been well studied in COPD. We investigated whether ADAM9 is linked to COPD in humans and mice.

Methods: ADAM9 blood and lung levels were measured in COPD patients versus controls, and air- versus cigarette smoke (CS)-exposed wild-type (WT) mice. WT and *Adam9*$^{-/-}$ mice were exposed to air or CS for 1-6 months, and COPD-like lung pathologies were measured.

Results: ADAM9 staining was increased in lung epithelial cells and macrophages in smokers and even more so in COPD patients and correlated directly with pack-year smoking history and inversely with airflow obstruction and/or FEV_1 % predicted. Bronchial epithelial cell *ADAM9* mRNA levels were higher in COPD patients than controls and correlated directly with pack-year smoking history. Plasma, BALF and sputum ADAM9 levels were similar in COPD patients and controls. CS exposure increased Adam9 levels in WT murine lungs. *Adam9*$^{-/-}$ mice were protected from emphysema development, small airway fibrosis, and airway mucus metaplasia. CS-exposed *Adam9*$^{-/-}$ mice had reduced lung macrophage counts, alveolar septal cell apoptosis, lung elastin degradation, and shedding of VEGFR2 and EGFR in BALF samples. Recombinant ADAM9 sheds EGF and VEGF receptors from epithelial cells to reduce activation of the Akt pro-survival pathway and increase cellular apoptosis.

Conclusions: ADAM9 levels are increased in COPD lungs and linked to key clinical variables. Adam9 promotes emphysema development, and large and small airway disease in mice. Inhibition of ADAM9 could be a therapeutic approach for multiple COPD phenotypes.

Key words: Emphysema; small airway fibrosis; mucus metaplasia; inflammation; growth factor receptor;

Abstract word count: 246

AJRCCM Articles in Press. Published on 04-June-2018 as 10.1164/rccm.201711-2300OC

Introduction

Chronic obstructive pulmonary disease (COPD) is the third leading cause of death worldwide[1]. The main risk factor for COPD is exposure to cigarette smoke (CS). Pulmonary emphysema develops following CS-induced injury to alveolar septal cells[2] and proteinase-mediated injury to the lung extracellular matrix[3]. CS exposure also induces small airway fibrosis[4], and mucus hyper-secretion, and proteinases have been implicated in these processes[3,5].

Among the proteinase culprits implicated in COPD, most is known about the contributions of serine and cysteine proteinases and matrix metalloproteinases (MMPs)[3]. Little is known about the contributions of the ADAMs subfamily of metalloproteinases to the pathogenesis COPD. ADAMs are type-I multi-domain transmembrane proteinases that can contain: 1) a pro-domain which maintains latency of the catalytic domain; 2) a metalloproteinase domain; 3) a disintegrin domain that can bind to integrins; 4) a cysteine-rich domain; 5) an epidermal growth factor (EGF)-like domain; 6) a membrane-spanning domain; and 7) a cytoplasmic tail which may regulate cellular signaling[6]. There is only one prior study that measured the expression of an ADAM in COPD samples. This study reported that sputum ADAM8 levels were higher in COPD patients than healthy controls[7].

ADAM9 is expressed by cells implicated in COPD including PMNs, macrophages, and epithelial cells[8-10], and contains all of the domains listed above. Although ADAM9 promotes injury to the alveolar-capillary barrier during acute lung injury in mice[8], little else is known about its contributions to lung diseases. We tested the hypotheses that: 1) ADAM9 levels are increased in blood and/or lung samples from COPD patients, and CS-exposed mice; and 2) ADAM9 promotes the development of COPD-like lung pathologies in CS-exposed mice.

Materials and Methods

See Online Supplement for details.

Human Subjects

Human studies were approved by institutional review boards in the USA and UK. Four cohort types were studied (lung immunostaining, sputum, plasma, and bronchoscopy cohorts). **Tables 1-2** and **E1-E3** and **E5** show the demographic and clinical data on these cohorts.

Immunostaining of lung sections for ADAM9: Lung sections from COPD patients and controls were double immunostained in red for markers of alveolar macrophages (CD163) or epithelial cells (pancytokeratin; PanCK), and in green for ADAM9. Lung sections were double immunostained for ADAM9 and EGFR or VEGFR2.

ADAM9 steady state mRNA levels in bronchial brushings from the bronchoscopy cohort: See Online Supplement.

ADAM9 bronchoalveolar lavage fluid (BALF), plasma, and sputum levels: Soluble ADAM9 (sADAM9) levels were measured with an ELISA.

Animal and *In Vitro* Experiments

Studies of mice were approved by the local Institutional Animal Care and Use Committee.

CS exposures: Adult C57BL/6 strain WT and *Adam9*$^{-/-}$ mice were exposed to air or whole-body CS for 2 h/day on 6 days/week for 1-6 months[11].

Adam9 levels in WT murine lungs: Adam9 levels were measured using quantitative real-time PCR or an ELISA.

Emphysema and small airway fibrosis: Distal airspace size and fibrosis around small airways were measured on lung sections using morphometry methods[11].

AJRCCM Articles in Press. Published on 04-June-2018 as 10.1164/rccm.201711-2300OC

Airway Muc5ac staining and α-smooth muscle actin (α-SMA): Murine lung sections were immunostained for airway epithelial Muc5ac[12] and α-SMA (a myofibroblast marker).

Lung inflammation: BAL leukocytes were counted and pro- and anti-inflammatory mediators and tissue inhibitor of metalloproteinases-3 (Timp-3) protein levels were measured in lung samples using ELISAs.

Apoptosis of alveolar macrophages: Alveolar macrophages from air- or CS-exposed WT and *Adam9*$^{-/-}$ mice were immunostained for active caspase-3.

Lung elastin degradation: Desmosine (a marker of elastin degradation) was quantified in BALF and sera using an ELISA.

Alveolar septal cell death: Lung sections were immunostained for TUNEL-positive cells.

Active caspase-3 levels in lung epithelial cells and bone marrow-derived macrophages (BMDMs): WT and *Adam9*$^{-/-}$ alveolar epithelial cells or BMDMs were exposed to 7.5% or 20% cigarette smoke extract (CSE), respectively. Intracellular active caspase-3 levels were quantified[13] (see Online Supplement).

ADAM9-mediated shedding of epidermal growth factor receptor (EGFR) and vascular endothelial growth factor receptor-2 (VEGFR2): Soluble EGFR (sEGFR) and sVEGFR2 levels were measured in BALF and sera from mice using ELISAs. EGFR and VEGFR2 levels on alveolar septal cell surfaces were measured in lung sections using immunostaining. Human bronchial epithelial cell (HBECs) were incubated for 4 h with or without 10-60 nM active rhADAM9, with or without 10 μM GM6001 (a non-selective metalloproteinase inhibitor). Soluble EGFR and sVEGFR2 levels were measured in supernatants using ELISAs, and EGFR and VEGFR2 levels on HBEC surfaces were quantified using immunostaining.

ADAM9-induced apoptosis of HBECs: HBECs were incubated with or without 60 nM active rhADAM9 with or without 10 μM GM6001. Intracellular active caspase-3 levels were quantified[13].

Akt phosphorylation in murine lungs: See Online Supplement.

Statistics: Data are presented as box-plots showing medians and 25th and 75th percentiles and whiskers showing 10th and 90th percentiles (non-parametric data), or mean ± SD (parametric data), or scatter plots.

Human studies: Non-parametic data were analyzed using a One-Way ANOVA with Dunnett corrections for multiple comparisons. A multivariate regression model, with *ADAM9* gene expression as the dependent variable, identified clinical parameters for which to adjust *ADAM9* expression in correlation analyses. *ADAM9* expression was analyzed using a Bayesian regression model with informative normal priors on the correcting variables (age and pack-year smoking history). A more restrictive prior distribution was set on age as the multivariate analysis showed age correlated weakly with *ADAM9* expression. Contrasts were performed against the relevant group, and results reported as the posterior probability of no effect.

Murine studies: Data were analyzed with One-Way ANOVAs followed by pair-wise comparisons using Student's t-tests and Bonferroni corrections (parametic data), or Kruskal-Wallis One-Way ANOVA followed by pair-wise comparisons using Mann-Whitney U-tests with Bonferroni corrections (non-parametric data).

AJRCCM Articles in Press. Published on 04-June-2018 as 10.1164/rccm.201711-2300OC

Results

Human studies:

ADAM9 expression is increased in COPD lungs: **Table 1** shows the demographic and clinical characteristics of the lung immunostaining cohort. COPD patients had greater ADAM9 staining in alveolar (**Fig. 1A** and **1D**) and bronchial epithelial cells (**Fig. 1B** and **1E**) than smokers. Smokers had greater ADAM9 staining in both cell types than non-smokers. After correcting correlations for differences in age, sex, pack-year smoking history, and current smoker status, ADAM9 staining in both epithelial cell types correlated directly with pack-year smoking history (**Figs. E1A-E1B**) and inversely with FEV_1/FVC (**Figs. E1C-E1D)**. ADAM9 staining in bronchial epithelial cells (but not alveolar epithelial cells) correlated indirectly with FEV_1 percent predicted (**Fig. E1E-E1F**).

ADAM9 gene expression was quantified in bronchial brushings from a bronchoscopy cohort (most of whom were current smokers [**Table 2**]) using a microarray assay. *ADAM9* transcript levels were higher in bronchial brushings from COPD patients and symptomatic patients without airflow obstruction (GOLD 0) than non-smokers and smokers but were not related to GOLD stage (**Fig. 2A**). Real-time quantitative RT-PCR (qPCR) analysis confirmed that *ADAM9* transcript levels were higher in COPD versus control bronchial brushings (**Fig. 2B** and **Table E1**). There were significant direct correlations between *ADAM9* mRNA levels and MUC5AC staining in endo-bronchial biopsies, pack-year smoking history and quality-of-life scores (**Figs. 2C-2G**); and significant inverse correlations between *ADAM9* mRNA levels and FEV_1/FVC, FEV_1 percent predicted and MEF_{25} (**Figs. 2H-2J**). However, after adjusting *P* values for differences in age and pack-year smoking history between the groups (**Table 2**), *ADAM9* mRNA levels correlated significantly only with pack-year smoking history (**Table 3).**

COPD patients had greater ADAM9 staining in alveolar macrophages (**Fig. 1C and Fig. 1F)** than smokers. Smokers had greater ADAM9 staining in alveolar macrophages than non-smokers. After correcting correlations for differences in age, sex, pack-year smoking history, and current smoker status, ADAM9 staining in alveolar macrophages correlated directly with pack-year

smoking history (**Fig. E2A**) and inversely with FEV_1/FVC and FEV_1 percent predicted (**Fig. E2B-2C**). ADAM9 staining was detected in PMNs in COPD and smoker lungs (not shown), but this staining was not quantified as no/few PMNs were detected in non-smoker lungs. There were no significant differences in plasma, BALF, or sputum sADAM9 levels between COPD patients and controls (**Figs. E3A-E3C** and **Tables E2** and **E3**).

Murine studies:

Adam9 deficiency decreases multiple key COPD-like lung pathologies in CS-exposed mice: Exposing WT mice to CS increased both Adam9 transcript and protein lung levels within 1 month, and levels increased further after 2 and 6 months of CS exposure (**Figs. 3A-3B).** As Timp-3 is the only Timp that inhibits Adam9[14], lung Timp-3 protein levels were measured in WT mice. CS exposure increased lung Timp-3 levels, but levels peaked after 1 month of CS exposure (**Fig. 3C**) and Adam9: Timp-3 protein ratios increased after 6 months of CS exposure (**Fig. 3D**).

Unchallenged *Adam9*$^{-/-}$ mice have no abnormal phenotype[15]. When exposed to CS for 6 months, *Adam9*$^{-/-}$ mice were protected from emphysema development (**Figs. 4A-4B)**, small airway fibrosis (**Figs. 4C-4D**), and had fewer α-SMA-positive myofibroblasts around their small airways (**Fig. 4E**). *Adam9*$^{-/-}$ mice were also protected from CS-induced airway mucus cell metaplasia (**Figs. 4F-4G**).

Lung inflammation: Lung inflammation was measured in WT and *Adam9*$^{-/-}$ mice as this process promotes emphysema development, small airway remodeling, and mucus metaplasia[16-20]. Compared with WT mice, *Adam9*$^{-/-}$ mice had lower BAL total leukocyte and macrophage (**Figs. 5A-5B**) counts detectable after 1 month of CS exposure, lower PMN counts after 6 months CS exposure (**Fig. 5C**), but similar BAL lymphocyte counts (**Fig. 5D**). CS-exposed *Adam9*$^{-/-}$ mice had lower macrophage counts in lung sections than WT mice (**Figs. 5E-5F**).

Lung levels of cytokines and chemokines that regulate myeloid leukocyte recruitment, activation, and survival (Ccl-2, Ccl-3, Ccl-5, Cxcl-1, Cxcl-2, Tnf-α, Il-6, Il-1β, Gm-csf, M-csf, and

AJRCCM Articles in Press. Published on 04-June-2018 as 10.1164/rccm.201711-2300OC

G-csf), and anti-inflammatory mediators (Il-10 and Tgf-β) were measured in WT and *Adam9*$^{-/-}$ mice exposed to air or CS for 1 month. Lung levels of Ccl-2, Il-1β, Il-10, G-csf, and active Tgf-β were similar in CS-exposed WT and *Adam9*$^{-/-}$ mice (**Fig. E4**). Lung levels of Gm-csf, M-csf, Ccl-3, and Cxcl-2 were lower in CS-exposed *Adam9*$^{-/-}$ versus WT mice (**Figs. 6A-6D**). Thus, *Adam9* deficiency may decrease lung macrophage counts, in part, by reducing lung levels of mediators that promote macrophage recruitment and activation (Ccl-3) or survival (Gm-csf, M-csf).

Surprisingly, lung levels of Tnf-α, Il-6, Ccl-5 and Cxcl-1 (the murine ortholog of IL-8) were higher in CS-exposed *Adam9*$^{-/-}$ than WT mice (**Figs. 6E-6H**). However, it is unlikely that Adam9's metalloproteinase domain degrades these mediators in the lung, as active human ADAM9 did not degrade human CCL-5, IL-8, IL-6, or TNF-α *in vitro* (**Figs. E5A-E5E**).

To investigate whether *Adam9* deficiency reduces lung macrophage counts by increasing macrophage apoptosis rates, intracellular levels of active caspase-3 were measured in alveolar macrophages isolated from air- versus CS-exposed WT and *Adam9*$^{-/-}$ mice. CS-exposed *Adam9*$^{-/-}$ mice had higher rates of alveolar macrophage apoptosis than WT mice (**Fig. 7A**). Macrophages isolated from unchallenged WT and *Adam9*$^{-/-}$ were induced to undergo apoptosis *in vitro* by exposing them to CS extract (CSE). Intracellular active caspase-3 levels were similar in CSE-treated WT and *Adam9*$^{-/-}$ cells (**Fig. E6**). Thus, macrophage-derived Adam9 is unlikely to regulate CS-induced macrophage apoptosis.

Proteinase-mediated elastin degradation promotes emphysema development. ADAM9 degrades elastin *in vitro*[8]. BALF and serum levels of desmosine (a measure of elastin degradation) were lower in CS-exposed *Adam9*$^{-/-}$ mice versus WT mice (**Figs. 7B-7C**). Thus, Adam9 may promote emphysema development, in part, by degrading lung elastin.

Alveolar septal cell death: Alveolar septal cell death contributes to emphysema development[2]. CS-exposed *Adam9*$^{-/-}$ mice had reduced alveolar septal cell death rates (assessed as fewer TUNEL-positive alveolar septal cells) compared with WT mice (**Figs. 7D-7E**). CSE induced lower rates of apoptosis in lung epithelial cells isolated from naive *Adam9*$^{-/-}$ versus WT mice (**Fig. 7F**).

Signaling of ligands *via* EGFR and VEGFR2 promotes the survival of alveolar septal cells[21,22]. Blocking VEGFR2 signaling in rats induces alveolar septal cell death and emphysema development[2]. To determine whether Adam9 promotes alveolar septal cell death by shedding their EGFR and/or VEGFR2, BALF soluble EGFR (sEGFR) and sVEGFR2 levels were measured. CS-exposed *Adam9*$^{-/-}$ mice had lower BALF sEGFR (**Fig. 8A)** and sVEGFR2 (**Fig. 8D**) levels than WT mice. Residual surface EGFR (**Figs. 8B-8C)** and VEGFR2 (**Figs. 8E-8F**) levels were higher on alveolar septal cells in CS-exposed *Adam9*$^{-/-}$ mice versus WT lungs.

Incubating HBECs from healthy subjects with active rhADAM9 *in vitro* decreased their surface EGFR (**Figs. 9A-9B**), and VEGFR2 (**Figs. 10A-10B**) staining, and increased sEGFR (**Fig. 9C**) and sVEGFR2 (**Fig. 10C**) levels in culture supernatants. A non-selective small-molecule metalloproteinase inhibitor (GM6001) blocked ADAM9-mediated shedding of both receptors from HBECs (**Figs. 9D-9E, 10D-10E**). Incubating HBECs with rhADAM9 increased intracellular active caspase-3 levels, which was rescued by GM6001 (**Fig. 10F**).

HBECs from COPD patients had greater ADAM9 surface staining, but lower EGFR and VEGFR2 surface staining than HBECs from controls (**Figs. 11A-11D;** and **Table E4)**. The greater ADAM9 staining detected in bronchial and alveolar epithelial cells in COPD versus control lung sections was associated with lower staining for EGFR and VEGFR2 in the same cells (**Fig. E7;** and **Table E5**).

Signaling through EGFR and VEGFR2 activates (phosphorylates) intracellular phosphoinositide 3-kinase (PI3K) and Akt inducing downstream activation of pro-survival signaling pathways[23]. Incubating HBECs with active rhADAM9 reduced phospho-Ser^{473}Akt levels. Inhibiting ADAM9 with GM6001 rescued activation (phosphorylation) of Akt (**Fig. 12A-12B**). HBECs from COPD patients had lower phospho-Ser^{473}Akt levels than cells from controls (**Figs. 12C-12D**). Total Akt lung levels were similar but phospho-Ser^{473}Akt levels were higher in CS-exposed *Adam9*$^{-/-}$ versus WT lungs (**Fig. 12E-12F**). Thus, ADAM9 proteolytically inactivates

AJRCCM Articles in Press. Published on 04-June-2018 as 10.1164/rccm.201711-2300OC

EGFR- and VEGFR2-triggered Akt pro-survival signaling in alveolar septal cells to promote emphysema development.

Discussion

This study identifies ADAM9 as new culprit in COPD, and the first proteinase linked to five key COPD-like pulmonary pathologies (lung inflammation, alveolar septal cell apoptosis, emphysema, small airway fibrosis, and mucus cell metaplasia,) in CS-exposed mice. ADAM9 immunostaining was increased in lung epithelial cells and macrophages in smokers and even more so in COPD patients. *ADAM9* gene expression was increased in bronchial brushings from COPD patients. ADAM9 expression in the human lung correlated directly with pack-year smoking history and/or inversely with pulmonary function parameters. Our study provides novel mechanistic insights into Adam9's contributions to COPD, as *Adam9*$^{-/-}$ mice have reduced CS-induced lung inflammation, elastin degradation, and alveolar septal cell apoptosis. Adam9 is also the first sheddase of EGFR and VEGFR2 identified in a murine model of COPD. Thus, strategies that reduce ADAM9 lung levels may limit the progression of emphysema, small airway disease, and chronic bronchitis.

Although ADAM9 expression is increased in lung macrophages in mice with acute lung injury[8,24], CS exposure increased lung levels of Adam9 and also Timp-3 (the only Timp family member that inhibits Adam9[14]) in WT murine lungs. However, chronic CS exposure increased lung Adam9:Timp-3 protein ratios, suggesting that active Adam9 is available in the lung to degrade elastin and cleave VEFGR2 and EGFR from alveolar septal cell surfaces.

ADAM9 expression has not been studied previously in patients with COPD or other chronic lung diseases. Increases in ADAM9 expression in lung macrophages and epithelial cells, and bronchial brushings were related to the presence of COPD but not COPD severity. ADAM9 protein and transcript levels correlated directly with pack-year smoking history. ADAM9 protein levels in macrophages and epithelial cells correlated inversely with airflow obstruction and percent predicted FEV_1 albeit in a small cohort. Gene expression in COPD lungs is generally most strongly correlated with current smoker status[25]. However, there was no relationship between current smoker status and ADAM9 expression as: 1) smokers (predominantly current smokers) in the bronchial brushings cohort had similar *ADAM9* gene expression levels as non-smokers; and 2) smokers in our lung

AJRCCM Articles in Press. Published on 04-June-2018 as 10.1164/rccm.201711-2300OC

immunostaining cohort (predominantly former smokers) had higher ADAM9 staining in epithelial cells and macrophages than non-smokers. Pro-inflammatory mediators increase ADAM9 expression in cell cultures[8], and pro-inflammatory signals generated in the lungs of former smokers with and without COPD may drive the increased ADAM9 immunostaining detected in their lungs.

Genetic and/or epigenetic processes may promote the increased ADAM9 expression in COPD lungs. Single-nucleotide polymorphisms in the *ADAM9* locus are associated with cone-rod dystrophy[26], but have not been linked to COPD. Although hyper-methylation of the *ADAM9* locus is linked to malignant transformation of mesenchymal stem cells[27], the methylation status of the *ADAM9* locus has not been examined in COPD lungs. MicroRNAs (miRNAs) regulate gene transcription in COPD lungs[28]. Expression of miR-126 is reduced in COPD lung epithelial cells[29], and *ADAM9* is a key target of miR-126[30]. Future studies will determine whether reduced miRNA-126 expression regulates *ADAM9* expression in COPD lungs.

sADAM9 isoforms have not been reported previously in plasma or lung samples, but have been detected in cell cultures[8,31] and are likely generated by shedding of ADAM9 from leukocytes or epithelial cells[8]. The sADAM9 isoforms we detected in COPD plasma, BALF, and sputum samples are unlikely to be a useful biomarker for COPD development or progression as sADAM9 levels were similar in COPD patients and controls.

Emphysema: Adam9 likely promotes emphysema development in mice by several mechanisms (**Fig. 13**). Adam9 may directly degrade lung elastin to cause loss of the alveolar walls, as human ADAM9 degrades elastin *in vitro*[8], and CS-exposed *Adam9*$^{-/-}$ mice had reduced lung elastin degradation. Adam9 may also promote emphysema development by increasing lung macrophage accumulation as: 1) lung macrophage counts were lower in CS-exposed *Adam9*$^{-/-}$ mice than WT mice; 2) macrophages are required for emphysema development in CS-exposed mice[16,17]; and 3) lung inflammation contributes to lung injury in COPD patients[32]. Macrophage-derived Adam9 is unlikely to regulate lung macrophage counts in CS-exposed lungs by: 1) modulating monocyte trans-endothelial migration as Adam9 is not essential for monocyte migration into the

lungs in other models[8]; or 2) inhibiting macrophage apoptosis as CSE-induced similar rates of apoptosis in WT and *Adam9*$^{-/-}$ macrophages *in vitro*. Adam9 may increase lung macrophage accumulation by: 1) increasing lung levels of cytokines that promote monocyte chemotaxis (Ccl-3); and 2) reducing macrophage apoptosis by increasing lung levels of growth factors that promote macrophage survival as Gm-csf, M-csf levels were lower in CS-exposed *Adam9*$^{-/-}$ lungs.

Adam9 may also promote emphysema development by increasing alveolar septal cell apoptosis. Apoptosis of alveolar epithelial and endothelial cells is driven by loss of signaling *via* EGFR and VEGFs and their receptors[2,22]. Pharmacologic blockade of VEGF receptors induces alveolar septal cell apoptosis and emphysema in rodents[2], but EGFR inhibitors have not been studied in rodent emphysema models. VEGFR2 levels are decreased in COPD lungs[33], but the mechanisms involved were not identified. Herein, we identify ADAM9 as a VEGFR2 and EGFR sheddase *in vitro* and in CS-exposed mice. It is noteworthy that there was increased ADAM9 staining associated with decreased VEGFR2 and EGFR staining in alveolar septal cells in COPD lungs. EGFR and VEGFR2 signaling promote cellular survival by activating the PI3K-Akt pathway[34], and increased activation of this pathway was detected in CS-exposed *Adam9*$^{-/-}$ versus WT lungs. Although MMPs cleave the EGFR and VEGFR2 in other models[35,36], ADAM9 is the first proteinase identified that sheds EGFR and VEGFR2 in CS-exposed mice.

Small airway fibrosis: Small airway fibrosis contributes significantly to airflow obstruction and FEV_1 decline in COPD patients[4], and it is noteworthy that bronchial epithelial cell ADAM9 staining correlated inversely with airflow obstruction and % predicted FEV_1. Activation of growth factors that drive deposition of interstitial collagen by airway myofibroblasts is linked to small airway fibrosis[37]. Although other proteinases proteolytically activate latent Tgf-β[38,39], CS-exposed *Adam9*$^{-/-}$ mice were protected from small airway fibrosis in a Tgf-β-independent fashion, as CS-exposed WT and *Adam9*$^{-/-}$ mice had similar lung levels of active Tgf-β. Adam9 may promote small airway fibrosis by activating fibroblasts as ADAM9 is expressed by fibroblasts and regulates fibroblast adhesion[40], and reduced numbers of α-SMA-positive myofibroblasts were detected around

AJRCCM Articles in Press. Published on 04-June-2018 as 10.1164/rccm.201711-2300OC

the small airways of CS-exposed *Adam9*$^{-/-}$ mice.

Adam9 may also promote small airway fibrosis in CS-exposed mice by increasing lung inflammation as macrophage products (including MMPs) promote small airway fibrosis in CS-exposed rodents[5,19]. Adam9 may also induce M2 polarization of macrophages to promote small airway fibrosis[41].

Mucus metaplasia: Mucus metaplasia occurs in the large airways of COPD patients and contributes to the chronic bronchitis phenotype which is associated with high morbidity, poorer quality-of-life scores, increased rate of decline in FEV_1, more frequent exacerbations, and higher mortality rates[42]. ADAM9 may promote the chronic bronchitis phenotype as: 1) CS-exposed *Adam9*$^{-/-}$ mice had reduced mucus cell metaplasia; and 2) *ADAM9* expression bronchial brushings was higher in smokers with symptoms of cough and sputum (GOLD stage 0) than asymptomatic smokers. Future studies will measure ADAM9 expression in samples from patients with chronic bronchitis.

Mucin synthesis and goblet cell hyperplasia are induced by EGFR ligands activating this receptor[43]. ADAM-10 and -17 increase EGFR activation in epithelial cells *in vitro* by shedding (and thereby activating) EGFR ligands[44,45]. Adam9 likely regulates mucin synthesis by an EGFR-independent mechanism as Adam9 sheds the EGFR from epithelial cell surfaces. Mucin synthesis is also induced by TNF-α and IL-1β signaling[46,47], and other ADAMs and MMPs shed and activate latent pro-TNF-α from macrophage surfaces and activate pro-IL-1β[48-50]. However, lung levels of these cytokines were not reduced in CS-exposed *Adam9*$^{-/-}$ mice. Thus, it is unlikely that Adam9 induces mucin expression by proteolytically activating these mediators.

Limitations of this study: Small cohorts of COPD patients and controls were studied, and we may not have identified all possible confounding factors. Studies of larger COPD cohorts enriched for individual COPD phenotypes are needed to confirm our results. ADAM9 activity was not measured in clinical samples, due to the lack of available substrates that are selectively cleaved by ADAM9, and inhibitors that selectively inhibit ADAM9. Our murine studies employed only a loss-

of-function approach. Some of our findings could be due to compensatory changes in lung levels of other proteinases in *Adam9*$^{-/-}$ mice, rather than direct effects of Adam9. We did not fully elucidate the mechanisms by which Adam9 regulates small airway fibrosis and airway mucus cell metaplasia.

Conclusions: Herein, we identify ADAM9 as a novel proteinase culprit in COPD. Unlike other proteinases studied in murine models to date, Adam9 promotes the development of airspace, and large and small airway disease. Strategies to inhibit ADAM9 activity or reduce its expression in the lung could limit the progression of several key COPD phenotypes that are associated with high morbidity and mortality.

AJRCCM Articles in Press. Published on 04-June-2018 as 10.1164/rccm.201711-2300OC

Figure legends

***Figure 1: ADAM9 expression is increased in epithelial cells and alveolar macrophages (AMs) in COPD lungs*: A-C** show representative lung sections from non-smoker controls, smokers without COPD, and COPD patients (GOLD stages I-II and III-IV) that were double immunostained with a red fluorophore (left panels) for markers of airway epithelial cells (pan-cytokeratin; pan-CK in **A** and **B**) or a marker of macrophages (CD163 in **C**), and with a green fluorophore for ADAM9 (middle panels in **A-C**). Nuclei in the sections were counterstained blue using 4',6-diamidino-2-phenylindole (DAPI). The sections were examined using a confocal microscope. Merged images are shown in the right panels in **A, B,** and **C** (magnification in **A** and **B** is x 400, in **C** is x 1000). Lung sections from a non-smoker were stained with a red fluorophore and non-immune murine (Ms) IgG or non-immune rat IgG and with a green fluorophore and non-immune rabbit (Rb) IgG as controls (bottom panels). The images shown are representative of 6-9 subjects/group. In **D** and **E**, ADAM9-positive cells were quantified in alveolar (**D**) and bronchial (**E**) epithelial cells using MetaMorph software. In **F**, the percentage of alveolar macrophages that were positively stained for ADAM9 was quantified in 10 randomly acquired microscopic fields. The boxes show the medians and 25^{th} and 75^{th} percentiles, and the whiskers show the 10^{th} and 90^{th} percentiles. In **D-F**, data were analyzed using a One-Way ANOVA followed by Dunnett corrections for multiple comparisons. In **D-F**, *, $P < 0.05$; **, $P < 0.001$ versus non-smokers or the group indicated (n = 6-9 subjects/group).

Figure 2: Correlations between ADAM9 gene expression in human bronchial brushing cells and clinical parameters: In **A**, *ADAM9* mRNA levels were measured using a microarray assay in bronchial brushing cells from non-smoker controls (n = 12), smoker controls (n = 17), and GOLD stage 0 (n = 18), GOLD stage I (n = 10), and GOLD stage II-IV (n = 13) COPD patients. The bars show the mean (± SD). Data were analyzed using a Bayesian linear regression adjusting for age and pack-year smoking history. *, Posterior Probability of no effect (*PP)* < 0.05; **, *PP* < 0.001 versus non-smoker controls or the group indicated. In **B**, *ADAM9* steady state mRNA levels were measured in bronchial brushing cells from 14 non-smoker controls, 15 smoker controls, and 17 GOLD stage 0, 8 GOLD stage I, and 13 GOLD stage II-IV COPD patients in the bronchoscopy cohort using real-

time quantitative RT-PCR. The boxes in the box-plots show the medians and 25th and 75th percentiles, and the whiskers show the 10th and 90th percentiles. Data were analyzed using a Bayesian linear regression adjusting for differences in age and pack-year smoking history. *, $PP < 0.05$ and **, $PP < 0.001$ versus non-smoker controls or the group indicated (*PP* is the posterior probability of no effect). **C- I** show correlations between *ADAM9* gene expression in human bronchial brushing cells and clinical parameters including: MUC5AC mucin staining in endo-bronchial biopsies from the same subjects (**C;** n = 50); pack-year smoking history (**D**; n = 67); St George's respiratory questionnaire (SGQR) quality-of-life total, symptom, and activity scores (**E-G**; n = 52); mean expiratory flow at 25% FVC (MEF_{25}; **H**, n = 62); FEV_1 percent predicted (**I**, n = 62) and FEV_1/FVC (**J**, n = 62). Data were analyzed using multivariate linear regression with *ADAM9* gene expression in human bronchial brushing cells as dependent variable and corresponding clinical parameter as well as relevant correction parameters (pack-year smoking history and age) as independent variables. $P < 0.05$ was considered to be statistically significant.

Figure 3: CS exposure induces the expression of Adam9 in murine lungs: In **A**, *Adam9* mRNA levels were measured in lungs from WT mice exposed to air (n = 20) or CS for 1 month (n = 10), 2 months (n = 10), or 6 months (n = 9) using real time RT-PCR. In **B**, Adam9 protein levels were measured in lungs from WT mice exposed to air (n = 22) or CS for 1 month (n = 11), 2 months (n = 14), or 6 months (n = 9) using an ELISA. In **C**, Timp-3 protein levels were measured in lungs from WT mice exposed to air (n = 8) or CS for 1 month (n = 8), 2 months (n = 9), or 6 months (n = 9) using an ELISA. In **D**, Adam9: Timp-3 protein ratios that were analyzed on the same lungs from WT mice exposed to air (n = 8) or CS for 1 month (n = 8), 2 months (n = 9), or 6 months (n = 9) were calculated. The boxes in the box-plots show the medians and 25th and 75th percentiles, and the whiskers show the 10th and 90th percentiles. Data were analyzed using a Kruskal-Wallis One-Way ANOVA followed by pair-wise testing with Mann-Whitney U tests and Bonferroni corrections. *, $P < 0.01$; **, $P < 0.001$ versus air-exposed controls or the group indicated.

AJRCCM Articles in Press. Published on 04-June-2018 as 10.1164/rccm.201711-2300OC

***Figure 4: Adam9 deficiency decreases emphysema development, small airway fibrosis, and mucus cell metaplasia in CS-exposed mice*:** In **A-G**, adult *Adam9*$^{-/-}$ mice and WT mice were exposed to air or CS 6 days-a-week for 6 months. **A:** Images of Gill's-stained inflated lung sections from mice (magnification X 200). **B:** Box-plots of alveolar chord lengths as a measure of airspace enlargement. The boxes show the medians and 25th and 75th percentiles, and the whiskers show the 10th and 90th percentiles for 6-11 air-exposed mice per group and 10-11 CS-exposed mice per group. Data were analyzed using a Kruskal-Wallis One-Way ANOVA followed by pair-wise testing with Mann Whitney U tests and Bonferroni corrections. *, $P < 0.017$ versus the same genotype exposed to air or the group indicated. **C** shows representative images of extracellular matrix (ECM) deposition around small airways (300-699 μm in diameter) in Masson Trichrome-stained lung sections from WT and *Adam9*$^{-/-}$ mice exposed to air or CS for 6 months. **D:** The thickness of the ECM protein layer deposited around small airways was quantified, as described in the Online Supplement. Boxes in the box-plots show the median values and 25th and 75th percentiles, and whiskers show the 10th and 90th percentiles from 8-10 air-exposed mice/group and 8-9 CS-exposed mice/group. Data were analyzed using a Kruskal-Wallis One-Way ANOVA followed by pair-wise testing with Mann-Whitney U tests with Bonferroni corrections. *, $P < 0.017$ versus air-exposed mice belonging to the same genotype or the group indicated. **E**: Scatter-plots of α-smooth muscle actin (α-SMA) staining that was quantified per unit area of airway wall on airways having a luminal diameter of 300-699 μm using MetaMorph software (4-5 air-exposed mice/group and 7-8 CS-exposed mice/group. Data were analyzed using a Kruskal-Wallis One-Way ANOVA followed by pair-wise testing with Mann-Whitney U tests and Bonferroni corrections. *, $P < 0.017$ versus air-exposed mice belonging to the same genotype or the group indicated. **F:** Images of immunofluorescence staining for bronchial epithelial Muc5ac (stained in green) in the lungs of CS-exposed WT and *Adam9*$^{-/-}$ mice that are representative of 5-7 mice/group. A section of lung from a CS-exposed WT mouse stained with a non-immune murine (Ms) IgG is shown (right panel). Air-exposed WT and *Adam9*$^{-/-}$ mice had minimal staining for Muc5ac in bronchial epithelial cells (data not shown). **G**: Muc5ac staining was quantified per unit area of bronchial epithelium using MetaMorph software. Boxes in the box-plots

show the median values and 25th and 75th percentiles, and whiskers show the 10th and 90th percentiles for mice exposed to air (n = 5/group) or CS (n =7/group) for 6 months. Data were analyzed using a Kruskal-Wallis One-Way ANOVA followed by pair-wise testing with Mann-Whitney U tests with post-hoc Bonferroni corrections. *, $P < 0.017$ versus air-exposed mice belonging to the same genotype or the group indicated.

***Figure 5: Lung inflammation is decreased in CS-exposed Adam9$^{-/-}$ mice*:** WT and *Adam9*$^{-/-}$ mice were exposed to air or CS for 1-6 months. Absolute numbers of all leukocytes (**A**), macrophages (**B**), PMNs (**C**), and lymphocytes (**D**) were counted in bronchoalveolar lavage (BAL) samples. Boxes in the box-plots show the median values and 25th and 75th percentiles, and whiskers show the 10th and 90th percentiles for 8-9 air-exposed mice/group, 10-12 mice exposed to CS for 1 month per group, 15-22 mice exposed to CS for 2 months per group, 5-9 mice exposed to CS for 3 months per group, and 5 mice exposed to CS for 6 months per group. Data were analyzed using a Kruskal-Wallis One-Way ANOVA followed by pair-wise testing with Mann-Whitney U tests with Bonferroni corrections for multiple comparisons. *, $P < 0.008$; and **, $P < 0.001$ versus the group indicated. **E:** Images of lung sections from WT and *Adam9*$^{-/-}$ mice that were exposed to air or CS for 6 months that were immunostained with a green fluorophore for CD68 (a marker of macrophages). The images shown are representative of 6-7 mice/group. A section of lung from a CS-exposed WT mouse stained with a non-immune primary murine (Ms) IgG is shown (right panel). In **F**, CD68 staining was quantified per unit area of alveolar wall using MetaMorph software. The bars show the mean (± SD) for 6 mice that were exposed to air per group, and 7 mice that were exposed to CS for 6 months per group. Data were analyzed using a One-Way ANOVA followed by pair-wise testing with Student's t-tests and Bonferroni corrections for multiple comparisons. *, $P < 0.017$ versus air-exposed mice belonging to the same genotype or the group indicated.

Figure 6: Lung levels of cytokines and chemokines in air- versus CS-exposed WT and Adam9$^{-/-}$ mice: WT and *Adam9*$^{-/-}$ mice were exposed to air or CS for 1 month, and lung levels of Gm-csf (**A**; n = 6-13 mice/group), M-csf (**B**; n = 8-12 mice/group), Ccl-3 (**C**; n = 13-17 mice/group), Cxcl-2 (**D**; n

AJRCCM Articles in Press. Published on 04-June-2018 as 10.1164/rccm.201711-2300OC

= 8-12 mice/group), Tnf-α (**E**; n = 10-11 mice/group), Il-6 (**F;** n = 10-11 mice/group), Ccl-5 (**G;** n = 8-9 mice/group), and Cxcl-2 (**H;** n = 8-10 mice/group) were measured in homogenates of lung samples using ELISA kits. Data were normalized to total protein levels measured on the same samples. Boxes in the box-plots show the median values and 25th and 75th percentiles, and whiskers show the 10th and 90th percentiles. Data were analyzed using a Kruskal-Wallis One-Way ANOVA followed by pair-wise testing with Mann-Whitney U tests with Bonferroni corrections for multiple comparisons. *, $P < 0.025$; and **, $P < 0.001$ versus air-exposed mice belonging to the same genotype or the group indicated.

***Figure 7: CS-exposed Adam9$^{-/-}$ mice have higher alveolar macrophage apoptosis rates, but lower lung elastin degradation, and alveolar septal cell death rates than CS-exposed WT mice*:** In **A-E,** WT and *Adam9$^{-/-}$* mice were exposed to air or CS for 1-6 months. **A**: Alveolar macrophages were isolated from the lungs of WT and *Adam9$^{-/-}$* mice that had been exposed to air or CS for 1 month using BAL. Immediately afterwards, the alveolar macrophages were fixed and then immunostained for intracellular active caspase-3. Staining was quantified, as described in the Online Supplement (n = 3 separate experiments). Data are mean ± SD. Data were analyzed using a Kruskal-Wallis One-Way ANOVA followed by pair-wise testing with Mann-Whitney U tests and Bonferroni corrections for multiple comparisons. *, $P < 0.025$ versus the group indicated. **B:** Desmosine levels were measured in bronchoalveolar lavage fluid (BALF) samples from WT and *Adam9$^{-/-}$* mice exposed to air (n = 5-6 mice/group), or CS for 1 month (n = 15 mice/group) or 3 months (n = 6 mice/group) using an ELISA. Boxes in the box-plots show the median values and 25th and 75th percentiles, and whiskers show the 10th and 90th percentiles. Data were analyzed using a Kruskal-Wallis One-Way ANOVA followed by pair-wise testing with Mann-Whitney U test and Bonferroni corrections for multiple comparisons. *, $P < 0.017$; and **, $P < 0.001$ versus the group indicated. **C:** Desmosine levels were measured in serum samples from WT and *Adam9$^{-/-}$* mice exposed to air (n = 5 mice/group) or CS (n = 11-12 mice/group) for 6 months using an ELISA. Data are mean ± SD. Data were analyzed using a One-Way ANOVA followed by pair-wise testing with Student's t-tests and Bonferroni corrections for multiple comparisons. *, $P < 0.025$ versus the group indicated. **D** shows

representative images of terminal deoxynucleotidyl transferase dUTP nick end labeling (TUNEL) staining on formalin-fixed lung sections from WT and *Adam9*$^{-/-}$ mice exposed to air or CS for 6 months. **E**: Alveolar septal cell death was measured as the number of TUNEL-positive alveolar septal cells per unit alveolar wall area. Data shown are mean (± SD) values from 3-6 mice/group. Data were analyzed using a One-Way ANOVA followed by pair-wise testing with Student's t-tests and Bonferroni corrections for multiple comparisons. *, $P < 0.017$ versus air-exposed mice belonging to the same genotype or the group indicated. **F**: Type-II alveolar epithelial cells were isolated from unchallenged WT and *Adam9*$^{-/-}$ mice, and exposed to 7.5% CSE for up to 48 h. Intracellular levels of active caspase-3 were measured using a quenched fluorogenic substrate, as described in the Online Supplement. Data are mean ± SD from 8 separate cell preparations. Data were analyzed using a One-Way ANOVA followed by pair-wise testing with Student's t-tests and Bonferroni corrections for multiple comparisons. *, $P < 0.01$; **, $P < 0.001$ versus the time points indicated.

Figure 8: Adam9 sheds EGFR and VEGFR2 in the lungs of CS-exposed mice: WT and *Adam9*$^{-/-}$ mice were exposed to air or CS for 1-3 months. Soluble EGFR levels (**A**; n= 5-12 mice/group) and soluble VEGFR2 levels (**D**; n= 5-15 mice/group) were quantified in bronchoalveolar lavage fluid (BALF) samples using ELISA. The boxes in the box-plots show the median values and 25th and 75th percentiles, and whiskers show the 10th and 90th percentiles. Data were analyzed using a Kruskal-Wallis One-Way ANOVA followed by pair-wise testing with Mann-Whitney U tests and Bonferroni corrections for multiple comparisons. *, $P < 0.017$; and **, $P < 0.001$ versus the group indicated. In **B** residual EGFR levels expressed on alveolar septal cell surfaces were assessed by immunostaining lung sections from WT and *Adam9*$^{-/-}$ mice exposed to air or CS for 6 months with a green fluorophore for EGFR. Nuclei were counterstained blue with DAPI. As a control, lung sections were stained with a non-immune rabbit (Rb) IgG (bottom panel). The merged images shown in **B** are representative of 3-5 mice per group. **C:** Scatter plots of residual surface EGFR staining that was quantified in alveolar septal cells in mice that were exposed to air (3-4 mice/group) or CS (4-5 mice/group) for 6 months using MetaMorph software. Data were analyzed using a Kruskal-Wallis

AJRCCM Articles in Press. Published on 04-June-2018 as 10.1164/rccm.201711-2300OC

One-Way ANOVA followed by pair-wise testing with Mann-Whitney U tests and Bonferroni corrections for multiple comparisons. *, $P < 0.025$; and **, $P < 0.001$ versus the group indicated. In **E** residual VEGFR2 levels expressed on alveolar septal cell surfaces were assessed by immunostaining lung sections from WT and *Adam9*$^{-/-}$ mice that were exposed to air or CS for 6 months with a green fluorophore for VEGFR2. Nuclei were counterstained blue with DAPI. As a control, lung sections were stained with a non-immune Rb IgG (bottom panel). The merged images shown in **E** are representative of 4-6 mice per group. **F**: Scatter plots of residual surface VEGFR2 staining quantified in alveolar septal cells in sections of lungs from mice that had been exposed to air (4-5 mice/group) or CS (5-6 mice/group) for 6 months. Data were analyzed using a Kruskal-Wallis One-Way ANOVA followed by pair-wise testing with Mann-Whitney U test and Bonferroni corrections for multiple comparisons. *, $P < 0.025$ versus the group indicated.

Figure 9: ADAM9 sheds EGFR from human bronchial epithelial cell (HBEC) surfaces: **A**: HBECs from control subjects without COPD were grown to confluence on chamber slides and incubated with or without 10-60 nM active recombinant human (rh)ADAM9 for 4 h at 37^{o}C. HBECs were fixed and immunostained with a green fluorophore for cell surface-associated EGFR. As a control, cells not incubated with rhADAM9 were stained with a non-immune rabbit (Rb) IgG (right panel). DAPI counter-stained cells were examined using an epi-fluorescence microscope. The merged images shown in **A** are representative of 4 separate experiments. In **B**, residual levels of EGFR on the surface of HBECs were quantified, as described in the Online Supplement. The boxes in the box-plots show the median values and 25th and 75th percentiles, and whiskers show the 10th and 90th percentiles (n = 4 separate experiments). Data were analyzed using a Kruskal-Wallis One-Way ANOVA followed by pair-wise testing with Mann-Whitney U tests. *, $P < 0.029$; and **, $P < 0.001$ versus no rhADAM9 control or the group indicated. **C** shows soluble EGFR levels in cell-free supernatant samples from the same preparations shown in **A-B** measured using an ELISA. The boxes in the box-plots show the median values and 25th and 75th percentiles, and whiskers show the 10th and 90th percentiles (n = 5 separate experiments). Data were analyzed using a Kruskal-Wallis One-Way ANOVA followed by pair-wise testing with Mann-Whitney U tests. *, $P < 0.019$; **, $P < 0.001$

versus the group indicated. **D:** Images showing residual EGFR staining on the surface of HBECs that were incubated with or without 60 nM rhADAM9 with or without 2 μM or 10 μM GM6001 (a non-selective metalloproteinase inhibitor) for 4 h at 37°C. The right panel shows cells incubated without rhADAM9 that were stained with a non-immune rabbit (Rb) IgG. In **E**, residual EGFR levels on the surface of HBECs were quantified, as described in the Online Supplement. Data are mean ± SD from 3 separate experiments. Data were analyzed using a One-Way ANOVA followed by pair-wise testing with Student's t-tests. *, $P < 0.011$; and **, $P < 0.001$ versus the group indicated.

Figure 10: ADAM9 sheds VEGFR2 from human bronchial epithelial cell (HBEC) surfaces: **A**: HBECs from control subjects without COPD were grown to confluence on chamber slides and incubated with or without 10-60 nM active recombinant human (rh)ADAM9 for 4 h at 37^{o}C. HBECs were fixed and immunostained with a green fluorophore for cell surface-associated VEGFR2. As a control, cells not incubated with rhADAM9 were stained with a non-immune murine (Ms) IgG (right panel). The merged images shown in **A** are representative of 4 separate experiments. In **B**, residual levels of VEGFR2 on the surface of HBECs were quantified, as described in the Online Supplement. The boxes in the box-plots show the median values and 25th and 75th percentiles, and whiskers show the 10th and 90th percentiles (n = 4 separate experiments). Data were analyzed using a Kruskal-Wallis One-Way Analysis followed by pair-wise testing with Mann-Whitney U tests. *, $P < 0.029$; **, $P < 0.001$ versus no rhADAM9 control or the group indicated. **C**: Soluble VEGFR2 levels in cell-free supernatant samples from the same preparations shown in A-B were measured using an ELISA. The boxes in the box-plots show the median values and 25th and 75th percentiles, and whiskers show the 10th and 90th percentiles (n = 5 separate experiments). Data were analyzed using a Kruskal-Wallis One-Way ANOVA followed by pair-wise testing with Mann-Whitney U tests. *, $P < 0.011$; **, $P < 0.001$ versus the group indicated. **D:** Images of surface VEGFR2 staining on HBECs that were incubated with or without 60 nM rhADAM9 with or without 2 μM or 10 μM GM6001 (a non-selective small-molecule metalloproteinase inhibitor) for 4 h at 37°C. The right panel shows cells incubated without rhADAM9 that were stained with a non-immune murine (Ms) IgG. **E:** Residual EGFR levels on the surface of HBECs were quantified as described in the Online Supplement. Data

AJRCCM Articles in Press. Published on 04-June-2018 as 10.1164/rccm.201711-2300OC

are mean ± SD from 3 separate experiments. Data were analyzed using a One-Way ANOVA followed by pair-wise testing with Students t-tests. *, $P < 0.012$; and **, $P < 0.001$ versus the group indicated. In **F**, HBECs were grown to confluence on tissue culture plates and incubated with or without 60 nM active rhADAM9 at 37^{o}C for 4 h in the presence or absence of 10 μM GM6001 (a non-selective metalloproteinase inhibitor). Intracellular levels of active caspase-3 were measured using a quenched fluorogenic substrate, as described in the Online Supplement. Data are mean ± SD from 4 separate cell preparations. Data were analyzed using a One-Way ANOVA followed by pair-wise testing with Student's t-tests. *, $P < 0.029$ versus no rhADAM9 control or the group indicated.

Figure 11: Human bronchial epithelial cells (HBECs) from COPD patients have higher surface staining for ADAM9 and lower surface staining for EGFR and VEGFR2 than HBECs from controls. In **A-D**, primary HBECs from 3 COPD patients and 3 controls were grown to confluence on chamber slides. HBECs were fixed and immunostained with a green fluorophore for cell surface-associated ADAM9, EGFR, or VEGFR2, and the nuclei were counterstained blue with DAPI. Control cells were also stained with a primary non-immune rabbit (Rb) IgG or murine (Ms) IgG (right panels). The merged images shown in **A** are representative of 3 subjects/group. Cell surface levels of ADAM9 (in **B**), EGFR (in **C**), and VEGFR2 (in **D**) on HBECs were quantified on cells as described in the Online Supplement. Data are mean ± SD and data were analyzed using a One-Way ANOVA followed by pair-wise testing with Students t-tests. *, $P < 0.05$ versus control.

Figure 12: ADAM9 reduces activation (phosphorylation) of Akt. In **A-B**, HBECs were grown to confluence on tissue culture plates and incubated with or without 10-60 nM active rhADAM9 at 37^{o}C for 4 h in the presence or absence of 10 μM GM6001 (a non-selective metalloproteinase inhibitor). Phosphorylated Akt (p-Akt-Ser^{473}), total Akt (Akt), and a housekeeping control (β-Actin) were quantified in cell extracts using Western blotting and densitometry. The images of Western blots shown in **A** are representative of 5 separate experiments. **B:** The p-Akt-Ser^{473} signals were normalized to total Akt levels and expressed as a % of the no rhADAM9 control result. The bars show means ± SD (n = 5 separate experiments). Data were analyzed using a One-Way ANOVA

followed by pair-wise testing with Student's t-tests. *, $P < 0.05$; and **, $P < 0.001$ versus no rhADAM9 control or the group indicated. In **C-D**, primary HBECs from COPD patients and controls were grown to confluence on tissue culture plates. Phosphorylated Akt (p-Akt-Ser^{473}), total Akt (Akt), and a housekeeping control (β-Actin) were quantified in cell extracts using Western blotting and densitometry. The images of Western blots shown in **C** are representative of 3 separate experiments conducted from cells on 3 different controls and 3 different COPD patients. **D:** The p-Akt-Ser^{473} signals were normalized to total Akt levels and expressed as a % of the control result. The bars show means ± SD (3 cell preparations/group). Data were analyzed using a One-Way ANOVA followed by pair-wise testing with Student's t-tests. *, $P < 0.05$ versus control cells. In **E-F**, WT and *Adam9*$^{-/-}$ mice were exposed to air or CS for 3 months. Phosphorylated Akt (p-Akt-Ser^{473}), total Akt (Akt), and a housekeeping control (β-Actin) were quantified in homogenates of lung samples using Western blotting and densitometry. The p-Akt-Ser^{473} signals were normalized to total Akt levels and expressed as a % of the values for WT mice exposed to air. The images shown in **E** are representative of 6 mice per group. **F:** The bars show means ± SD (n = 6 mice/group). Data were analyzed using a One-Way ANOVA followed by pair-wise testing with Student's t-tests and Bonferroni corrections for multiple comparisons. *, $P < 0.0125$; **, $P < 0.001$ versus air-exposed mice belonging to the same genotype or the group indicated.

Figure 13: Cartoon illustrating the potential contributions of ADAM9 to different COPD phenotypes.

1. Inhaling cigarette smoke increases the expression of ADAM9 in lung macrophages and bronchial and alveolar epithelial cells either directly, or indirectly by generating pro-inflammatory mediators in the lungs that induce ADAM9 expression by these cells. 2. ADAM9 may directly degrade lung elastin to promote emphysema development. 3. Increases in lung macrophage counts increases lung elastin degradation further (by increasing the lung burden of macrophage-derived matrix metalloproteinases [MMPs]) to contribute to emphysema development. Increase in lung macrophage counts may also contribute to lung inflammation and injury by increasing the lung burden of macrophage-derived oxidants (that injure alveolar septal cells) and macrophage-derived pro-

AJRCCM Articles in Press. Published on 04-June-2018 as 10.1164/rccm.201711-2300OC

inflammatory mediators that amplify macrophage recruitment and activation (CCL-3) and survival (GM-CSF and M-CSF). 4. ADAM9 expressed by alveolar epithelial cells sheds EGFR and VEGFR2 from lung epithelial cells to promote alveolar septal cell death and emphysema development by reducing activation of the PI3K/Akt pro-survival pathway in alveolar septal cells. 5. Adam9 also promotes small airway fibrosis, in part, by increasing α-smooth muscle actin-positive fibroblasts in the small airways, or possibly by increasing airway inflammation. 6. Adam9 increases airway mucus cell metaplasia *via* mechanisms that remain to be elucidated. The scissors indicate processes in which ADAM9's metalloproteinase domain is likely to be involved. Abbreviations used: EGFR, epidermal growth factor receptor; GM-CSF, granulocyte-macrophage colony stimulating factor; M-CSF, macrophage colony stimulating factor; MMPs, matrix metalloproteinases; PI3K, phospho-inositide 3-kinase; VEGFR2, vascular endothelial growth factor receptor-2.

Table 1: Demographic and clinical characteristics of the human immunostaining cohort.

Characteristics	Non-smokers* (N = 9)	Smokers* (N = 8)	COPD GOLD stages I-II (N = 6)	COPD GOLD stages III-IV (N = 8)	*P* value‡
Number of males (%)	2 (22)	3 (37.5)	4 (67)	5 (62.5)	***NS***
Age (years)	64 (35-82)	69 (54-79)	65 (52-77)	64 (58-71)	***NS***‡
Pack-yrs. of smoking	0	34 (10-60)	54 (20-86)	42 (25-60)	***P* < 0.001**‖
Number of current smokers (%)	0 (0)	1 (12.5)	0 (0)	2 (25)	***NS***
FEV_1 (% of predicted)†	97 ± 23	81 ± 16	77 ± 15	28 ± 12	***P* < 0.001**§
FEV_1/FVC (% of predicted)†	76 (71-80)	83 (72-112)	58 (42-66)	44 (22-66)	***P* < 0.001**§§

The table shows the demographic and clinical characteristics of the COPD patients, smokers without COPD, and non-smoker controls who underwent either a lung biopsy, lung volume reduction surgery, or lung transplantation (see Online Supplement). COPD patients were sub-divided according to Global Initiative for Obstructive Lung Disease (GOLD) criteria.

Data are presented as median (interquartile range) for non-parametric data or mean ± SD for parametric data.

*Non-smokers were all never-smokers. Smokers were defined as subjects that had ≥ 10 pack-year smoking history. Current smokers were defined as active smokers at the time of the biopsy or surgery, or former smokers who had stopped smoking ≤ 1 year before the biopsy or surgery.

AJRCCM Articles in Press. Published on 04-June-2018 as 10.1164/rccm.201711-2300OC

[†]All COPD patients had forced expiratory volume in 1 second/ forced vital capacity ratio (FEV_1/FVC) < 0.7 whereas smokers without COPD and non-smoker controls had $FEV_1/FCV \geq 0.7$.

[‡]Categorical variables were analyzed with Chi-Square tests. Statistical analyses included One-Way ANOVA tests for continuous variables (age, FEV_1 % predicted, FEV_1/FCV, and pack/years) followed by pair-wise comparisons using Student's t-tests for parametric data or Mann-Whitney U tests for non-parametric data.

[ll] The pack/year smoking histories of the GOLD stage I-II and GOLD stage III-IV COPD groups were not significantly different from those of the smoker group ($P = 0.2$ for both comparisons). The pack/year smoking histories of the GOLD stage I-II and GOLD stage III-IV COPD groups and the smoker group were significantly different from those of the non-smoker group by design.

[§] The FEV_1 of the GOLD stage III-IV COPD group was significantly lower than that of the smoker and non-smoker groups ($P < 0.001$ for both comparisons). The FEV_1 of the GOLD stage I-II COPD group was not significantly different from that of the smoker and non-smoker groups ($P = 0.7$ and $P = 0.1$).

[§§] The FEV_1/FVC ratios of the GOLD stage III-IV COPD group were significantly lower than those of the smoker and non-smoker groups ($P = 0.002$ and $P = 0.001$, respectively). The FEV_1/FVC ratios of the GOLD stage I-II COPD group were significantly lower than those of the smoker and non-smoker groups ($P = 0.007$ and $P = 0.002$, respectively).

NS: not significant.

Table 2: Demographic and clinical characteristics of the bronchoscopy (bronchial brushings) cohort for microarray assays.

Characteristics	Non-smokers* (N = 12)	Smokers* (N = 17)	COPD GOLD stage 0* (N = 18)	COPD GOLD stage I* (N = 10)	COPD GOLD stages II-IV* (N = 13)	*P* value‡
Number of males (%)	6 (50)	7 (41.2)	7 (38.9)	6 (60)	9 (69.2)	***NS***
Age (years)	54 ± 8	44 ± 10	51 ± 7	59 ± 6	54 ± 7	***P* < 0.001**‡
Pack-yrs. of smoking	0	33 (10-59)	46 (19-160)	38 (0-53)	60 (30-86)	***P* < 0.001**†
Number of current smokers (%)	0 (0)	17 (100)	18 (100)	7 (70)	11 (85)	***P* < 0.001**¶
FEV_1 (% of predicted)	110 (92-120)	105 (88-130)	95 (76-130)	95 (85-100)	67 (25-79)	***P* < 0.001**§
FEV_1/FVC (% of predicted)	74 (70-83)	80 (72-90)	76 (70-82)	68 (60-70)	59 (30-69)	***P* < 0.001**§§

The table shows the demographic and clinical characteristics of the COPD patients, smokers without COPD, and never-smokers that underwent a bronchoscopy to obtain bronchial brushings and endobronchial biopsies for analysis of *ADAM9* mRNA levels and MUC5AC staining in epithelial cells, respectively. Data are presented as median (interquartile range) for non-parametric data or mean ± SD for parametric data.

AJRCCM Articles in Press. Published on 04-June-2018 as 10.1164/rccm.201711-2300OC

[*] Subjects were classified as non-smoker controls, smoker controls without COPD, and smokers with COPD. Only those smokers with normal lung function and a high resolution computed tomography thoracic scan showing no evidence of emphysema were included in the smoker group. The COPD subjects were further classified according to the criteria of the Global Initiative for Obstructive Lung Disease (GOLD) into three groups: GOLD stage 0 COPD [having a chronic cough and sputum production but normal spirometry (n = 18)]; GOLD stage I COPD, with or without cough and sputum production and with $FEV_1 \geq 80\%$ of predicted but FEV_1/FVC to <70% (n = 10); and GOLD stage II-IV COPD, with or without cough and sputum production but FEV_1 between 25% and 79% of predicted and $FEV_1/FVC<70\%$ (n = 13).

[‡] Categorical variables were analyzed with Chi-Square tests. Statistical analyses included One-Way ANOVA tests for continuous variables (age, FEV_1% predicted, FEV_1/FCV, and pack/years) followed by pair-wise comparisons using Student's t-tests (for parametric data) or Mann-Whitney U tests (for non-parametric data).

[ǂ] The ages of the COPD GOLD stages II-IV, GOLD stage I, and GOLD stage 0 groups were not significantly different from those of the non-smokers. The ages of the COPD GOLD stages II-IV, GOLD stage I and GOLD stage 0 groups were significantly older than those of the smokers ($P < 0.05$, $P < 0.001$, and $P < 0.05$, respectively).

[†] The pack/year smoking histories of the COPD GOLD stages II-IV, GOLD stage I, GOLD stage 0 and the smoker groups were significantly higher than those of the non-smokers by design. The smokers and GOLD 0 and GOLD I COPD patients were matched for pack-year smoking history. The GOLD stage II-IV COPD patients had a significantly greater pack-year smoking history than the smoker controls.

[¶]The proportions of current smokers in the smoker and COPD GOLD stage 0, I, and II-IV groups were significantly higher than that of the non-smoker group. However, the proportion of current smokers was similar in the smoker, and COPD GOLD stages 0, I, and II-IV groups.

[§] The FEV_1 of the COPD GOLD stages II-IV group was significantly lower than that of the smoker and non-smoker groups ($P < 0.001$ for both comparisons). The FEV_1 of the COPD GOLD stage I group was also significantly lower than that of the smoker and non-smoker groups ($P < 0.05$ for both comparisons). The FEV_1 of the COPD GOLD stage 0 group was not significantly different from that of the smoker and non-smoker groups ($P= 0.054$ and $P= 0.098$, respectively).

[§§]The FEV_1/FVC ratio of the COPD GOLD stages II-IV group was significantly lower than that of the smoker and non-smoker groups ($P < 0.001$ for both comparisons). The FEV_1/FVC ratio of the COPD GOLD stage I group was significantly lower than that of the smoker and non-smoker groups ($P < 0.001$ and $P < 0.05$, respectively). The FEV_1/FVC ratio of the COPD GOLD stage 0 group was significantly lower than that of the smoker group ($P < 0.05$), but was not significantly different from that of the non-smoker group ($P = 0.235$).

NS: not significant.

AJRCCM Articles in Press. Published on 04-June-2018 as 10.1164/rccm.201711-2300OC

Table 3: Correlations between *ADAM9* gene expression in bronchial brushings and clinical parameters after adjusting the *P* values for differences in age and pack-years of smoking.

Clinical Parameters	β (SE)*	β†	*P* value
Pack-years of smoking	0.007 (0.002)	0.438	***P* < 0.001**
SGRQ symptom score¶	0.005 (0.003)	0.264	***P* = 0.10**
SGRQ activity score¶	0.005 (0.003)	0.211	***P* = 0.18**
SGRQ total score¶	0.005 (0.004)	0.165	***P* = 0.30**
MUC5AC§	-0.005 (0.006)	-0.129	***P* = 0.43**
Pulmonary MEF_{25}	-0.001 (0.003)	-0.045	***P* = 0.75**
FEV_1	0.002 (0.003)	0.086	***P* = 0.55**
FEV_1/FVC	0.005 (0.006)	0.116	***P* = 0.39**

Bronchoscopies were performed on COPD patients, smokers without COPD, and never-smokers to obtain bronchial brushing samples for *ADAM9* gene expression analysis and endobronchial biopsies to immunostain airway epithelial cells for MUC5AC as described in the Online Supplement (n = 70 subjects).

Data were analyzed using R v3.4 for Windows (The R Foundation for Statistical Computing, Vienna, Austria). To identify the relevant clinical parameters to correct for, and a multivariate regression model was run with *ADAM9* gene expression as the dependent variable and all of the clinical parameters. Variable selection was performed by optimization of the Akaike Information Criterion (AIC). The final model retained only 6 clinical variables of which pack-year smoking history had the highest significance. Thus, subsequent analyses were corrected for differences in pack-year smoking history and also to difference in age.

¶ SGRQ; St. George's Respiratory Disease Questionnaire.

§ MUC5AC immunoperoxidase staining was quantified in the endobronchial biopsies from the same

COPD patients, smokers without COPD, and never-smokers from whom the bronchial brushings were obtained, as described in the Online Supplement.

* β coefficient and standard error (SE).

† β is the standardized regression coefficient which evaluates the relative significance of each independent variable in multiple linear analyses.

AJRCCM Articles in Press. Published on 04-June-2018 as 10.1164/rccm.201711-2300OC

References

1. Mannino, D. M. and A. S. Buist. 2007. Global burden of COPD: risk factors, prevalence, and future trends. *Lancet* 370:765-773.

2. Kasahara, Y., R. M. Tuder, L. Taraseviciene-Stewart, T. D. Le Cras, S. Abman, P. K. Hirth, J. Waltenberger, and N. F. Voelkel. 2000. Inhibition of VEGF receptors causes lung cell apoptosis and emphysema. *J.Clin.Invest* 106:1311-1319.

3. Owen, C. A. 2008. Roles for proteinases in the pathogenesis of chronic obstructive pulmonary disease. *Int.J.Chron.Obstruct.Pulmon.Dis.* 3:253-268.

4. Hogg, J. C., F. Chu, S. Utokaparch, R. Woods, W. M. Elliott, L. Buzatu, R. M. Cherniack, R. M. Rogers, F. C. Sciurba, H. O. Coxson, et al. 2004. The nature of small-airway obstruction in chronic obstructive pulmonary disease. *N.Engl.J.Med.* 350:2645-2653.

5. Churg, A., R. Wang, X. Wang, P. O. Onnervik, K. Thim, and J. L. Wright. 2007. Effect of an MMP-9/MMP-12 inhibitor on smoke-induced emphysema and airway remodelling in guinea pigs. *Thorax* 62:706-713.

6. Seals, D. F. and S. A. Courtneidge. 2003. The ADAMs family of metalloproteases: multidomain proteins with multiple functions. *Genes Dev.* 17:7-30.

7. Oreo, K. M., P. G. Gibson, J. L. Simpson, L. G. Wood, V. M. McDonald, and K. J. Baines. 2014. Sputum ADAM8 expression is increased in severe asthma and COPD. *Clin.Exp.Allergy* 44:342-352.

8. Roychaudhuri, R., A. H. Hergrueter, F. Polverino, M. E. Laucho-Contreras, K. Gupta, N. Borregaard, and C. A. Owen. 2014. ADAM9 is a novel product of polymorphonuclear neutrophils: regulation of expression and contributions to extracellular matrix protein degradation during acute lung injury. *J.Immunol.* 193:2469-2482.

9. Namba, K., M. Nishio, K. Mori, N. Miyamoto, M. Tsurudome, M. Ito, M. Kawano, A. Uchida, and Y. Ito. 2001. Involvement of ADAM9 in multinucleated giant cell formation of blood monocytes. *Cell Immunol.* 213:104-113.

10. Dijkstra, A., D. S. Postma, J. A. Noordhoek, M. E. Lodewijk, H. F. Kauffman, N. H. ten Hacken, and W. Timens. 2009. Expression of ADAMs ("a disintegrin and metalloprotease") in the human lung. *Virchows Arch.* 454:441-449.

11. Laucho-Contreras, M. E., K. L. Taylor, R. Mahadeva, S. S. Boukedes, and C. A. Owen. 2015. Automated Measurement of Pulmonary Emphysema and Small Airway Remodeling in Cigarette Smoke-exposed Mice. *J.Vis.Exp.*52236. doi: 10.3791/52236.

12. Laucho-Contreras, M. E., F. Polverino, K. Gupta, K. L. Taylor, E. Kelly, V. Pinto-Plata, M. Divo, N. Ashfaq, H. Petersen, B. Stripp, et al. 2015. Protective role for club cell secretory protein-16 (CC16) in the development of chronic obstructive pulmonary disease. *Eur.Respir.J.* 45:1544-1556.

13. Knolle, M. D., T. Nakajima, A. Hergrueter, K. Gupta, F. Polverino, V. J. Craig, S. E. Fyfe, M. Zahid, P. Permaul, M. Cernadas, et al. 2013. Adam8 limits the development of allergic airway inflammation in mice. *J.Immunol.* 190:6434-6449.

14. Maretzky, T., S. Swendeman, E. Mogollon, G. Weskamp, U. Sahin, K. Reiss, and C. P. Blobel. 2017. Characterization of the catalytic properties of the membrane-anchored metalloproteinase ADAM9 in cell-based assays. *Biochem.J.* 474:1467-1479.

15. Weskamp, G., H. Cai, T. A. Brodie, S. Higashyama, K. Manova, T. Ludwig, and C. P. Blobel. 2002. Mice lacking the metalloprotease-disintegrin MDC9 (ADAM9) have no evident major abnormalities during development or adult life. *Mol.Cell Biol* 22:1537-1544.

16. Ofulue, A. F. and M. Ko. 1999. Effects of depletion of neutrophils or macrophages on development of cigarette smoke-induced emphysema. *Am.J Physiol* 277:L97-105.

AJRCCM Articles in Press. Published on 04-June-2018 as 10.1164/rccm.201711-2300OC

17. Hautamaki, R. D., D. K. Kobayashi, R. M. Senior, and S. D. Shapiro. 1997. Requirement for macrophage elastase for cigarette smoke-induced emphysema in mice. *Science* 277:2002-2004.

18. Churg, A., C. V. Marshall, D. D. Sin, S. Bolton, S. Zhou, K. Thain, E. B. Cadogan, J. Maltby, M. G. Soars, P. R. Mallinder, et al. 2012. Late intervention with a myeloperoxidase inhibitor stops progression of experimental chronic obstructive pulmonary disease. *Am.J.Respir.Crit Care Med.* 185:34-43.

19. Churg, A., S. Zhou, X. Wang, R. Wang, and J. L. Wright. 2009. The role of interleukin-1beta in murine cigarette smoke-induced emphysema and small airway remodeling. *Am J Respir.Cell Mol.Biol* 40:482-490.

20. Kim, S. and J. A. Nadel. 2004. Role of neutrophils in mucus hypersecretion in COPD and implications for therapy. *Treat.Respir.Med.* 3:147-159.

21. Miettinen, P. J., J. E. Berger, J. Meneses, Y. Phung, R. A. Pedersen, Z. Werb, and R. Derynck. 1995. Epithelial immaturity and multiorgan failure in mice lacking epidermal growth factor receptor. *Nature* 376:337-341.

22. Morissette, M. C., J. Parent, and J. Milot. 2009. Alveolar epithelial and endothelial cell apoptosis in emphysema: what we know and what we need to know. *Int.J.Chron.Obstruct.Pulmon.Dis.* 4:19-31.

23. Abid, M. R., S. Guo, T. Minami, K. C. Spokes, K. Ueki, C. Skurk, K. Walsh, and W. C. Aird. 2004. Vascular endothelial growth factor activates PI3K/Akt/forkhead signaling in endothelial cells. *Arterioscler.Thromb.Vasc.Biol.* 24:294-300.

24. Weskamp, G., J. Kratzschmar, M. S. Reid, and C. P. Blobel. 1996. MDC9, a widely expressed cellular disintegrin containing cytoplasmic SH3 ligand domains. *J Cell Biol.* 132:717-726.

25. Zeskind, J. E., M. E. Lenburg, and A. Spira. 2008. Translating the COPD transcriptome: insights into pathogenesis and tools for clinical management. *Proc.Am.Thorac.Soc.* 5:834-841.

26. Parry, D. A., C. Toomes, L. Bida, M. Danciger, K. V. Towns, M. McKibbin, S. G. Jacobson, C. V. Logan, M. Ali, J. Bond, et al. 2009. Loss of the metalloprotease ADAM9 leads to cone-rod dystrophy in humans and retinal degeneration in mice. *Am.J.Hum.Genet.* 84:683-691.

27. Teng, I. W., P. C. Hou, K. D. Lee, P. Y. Chu, K. T. Yeh, V. X. Jin, M. J. Tseng, S. J. Tsai, Y. S. Chang, C. S. Wu, et al. 2011. Targeted methylation of two tumor suppressor genes is sufficient to transform mesenchymal stem cells into cancer stem/initiating cells. *Cancer Res.* 71:4653-4663.

28. Osei, E. T., L. Florez-Sampedro, W. Timens, D. S. Postma, I. H. Heijink, and C. A. Brandsma. 2015. Unravelling the complexity of COPD by microRNAs: it's a small world after all. *Eur.Respir.J.* 46:807-818.

29. Paschalaki, K. E., A. Zampetaki, J. R. Baker, M. A. Birrell, R. D. Starke, M. G. Belvisi, L. E. Donnelly, M. Mayr, A. M. Randi, and P. J. Barnes. 2017. Downregulation of MicroRNA-126 Augments DNA Damage Response in Cigarette Smokers and COPD Patients. *Am J Respir Crit Care Med. 2018 Mar 1;197(5):665-668.*

30. Liu, R., J. Gu, P. Jiang, Y. Zheng, X. Liu, X. Jiang, E. Huang, S. Xiong, F. Xu, G. Liu, et al. 2015. DNMT1-microRNA126 epigenetic circuit contributes to esophageal squamous cell carcinoma growth via ADAM9-EGFR-AKT signaling. *Clin.Cancer Res.* 21:854-863.

31. Mazzocca, A., R. Coppari, F. R. De, J. Y. Cho, T. A. Libermann, M. Pinzani, and A. Toker. 2005. A secreted form of ADAM9 promotes carcinoma invasion through tumor-stromal interactions. *Cancer Res.* 65:4728-4738.

32. Barnes, P. J. 2004. Alveolar macrophages as orchestrators of COPD. *COPD.* 1:59-70.

33. Kasahara, Y., R. M. Tuder, C. D. Cool, D. A. Lynch, S. C. Flores, and N. F. Voelkel. 2001. Endothelial cell death and decreased expression of vascular endothelial growth factor and

AJRCCM Articles in Press. Published on 04-June-2018 as 10.1164/rccm.201711-2300OC

vascular endothelial growth factor receptor 2 in emphysema. *Am.J.Respir.Crit Care Med.* 163:737-744.

34. Wee, P. and Z. Wang. 2017. Epidermal Growth Factor Receptor Cell Proliferation Signaling Pathways. *Cancers (Basel). 2017 May 17;9(5). pii: E52.*

35. Sanderson, M. P., S. Keller, A. Alonso, S. Riedle, P. J. Dempsey, and P. Altevogt. 2008. Generation of novel, secreted epidermal growth factor receptor (EGFR/ErbB1) isoforms via metalloprotease-dependent ectodomain shedding and exosome secretion. *J.Cell Biochem.* 103:1783-1797.

36. Basagiannis, D. and S. Christoforidis. 2016. Constitutive Endocytosis of VEGFR2 Protects the Receptor against Shedding. *J.Biol.Chem.* 291:16892-16903.

37. Churg, A., H. Tai, T. Coulthard, R. Wang, and J. L. Wright. 2006. Cigarette smoke drives small airway remodeling by induction of growth factors in the airway wall. *Am.J.Respir.Crit Care Med.* 174:1327-1334.

38. Yu, Q. and I. Stamenkovic. 2000. Cell surface-localized matrix metalloproteinase-9 proteolytically activates TGF-beta and promotes tumor invasion and angiogenesis. *Genes Dev.* 14:163-176.

39. Chua, F., S. E. Dunsmore, P. H. Clingen, S. E. Mutsaers, S. D. Shapiro, A. W. Segal, J. Roes, and G. J. Laurent. 2007. Mice lacking neutrophil elastase are resistant to bleomycin-induced pulmonary fibrosis. *Am.J.Pathol.* 170:65-74.

40. Zigrino, P., R. Nischt, and C. Mauch. 2011. The disintegrin-like and cysteine-rich domains of ADAM-9 mediate interactions between melanoma cells and fibroblasts. *J Biol.Chem.* 286:6801-6807.

41. Shaykhiev, R., A. Krause, J. Salit, Y. Strulovici-Barel, B. G. Harvey, T. P. O'Connor, and R. G. Crystal. 2009. Smoking-dependent reprogramming of alveolar macrophage polarization:

implication for pathogenesis of chronic obstructive pulmonary disease. *J.Immunol.* 183:2867-2883.

42. Lahousse, L., L. J. M. Seys, G. F. Joos, O. H. Franco, B. H. Stricker, and G. G. Brusselle. 2017. Epidemiology and impact of chronic bronchitis in chronic obstructive pulmonary disease. *Eur Respir J. 2017 Aug 10;50(2). pii: 1602470. doi: 10.1183/13993003.02470-2016.*

43. Burgel, P. R. and J. A. Nadel. 2004. Roles of epidermal growth factor receptor activation in epithelial cell repair and mucin production in airway epithelium. *Thorax* 59:992-996.

44. Lemjabbar, H. and C. Basbaum. 2002. Platelet-activating factor receptor and ADAM10 mediate responses to Staphylococcus aureus in epithelial cells. *Nat.Med.* 8:41-46.

45. Lemjabbar, H., D. Li, M. Gallup, S. Sidhu, E. Drori, and C. Basbaum. 2003. Tobacco smoke-induced lung cell proliferation mediated by tumor necrosis factor alpha-converting enzyme and amphiregulin. *J Biol Chem.* 278:26202-26207.

46. Lai, H. and D. F. Rogers. 2010. New pharmacotherapy for airway mucus hypersecretion in asthma and COPD: targeting intracellular signaling pathways. *J.Aerosol Med.Pulm.Drug Deliv.* 23:219-231.

47. Lee, S. U., M. H. Sung, H. W. Ryu, J. Lee, H. S. Kim, H. J. In, K. S. Ahn, H. J. Lee, H. K. Lee, D. H. Shin, et al. 2016. Verproside inhibits TNF-alpha-induced MUC5AC expression through suppression of the TNF-alpha/NF-kappaB pathway in human airway epithelial cells. *Cytokine* 77:168-175.

48. Horiuchi, K., T. Kimura, T. Miyamoto, H. Takaishi, Y. Okada, Y. Toyama, and C. P. Blobel. 2007. Cutting edge: TNF-alpha-converting enzyme (TACE/ADAM17) inactivation in mouse myeloid cells prevents lethality from endotoxin shock. *J.Immunol.* 179:2686-2689.

49. Owen, C. A. 2008. Leukocyte cell surface proteinases: regulation of expression, functions, and mechanisms of surface localization. *Int.J Biochem.Cell Biol* 40:1246-1272.

AJRCCM Articles in Press. Published on 04-June-2018 as 10.1164/rccm.201711-2300OC

50. Schonbeck, U., F. Mach, and P. Libby. 1998. Generation of biologically active IL-1b by matrix metalloproteinases: a novel caspase-1-independent pathway of IL-1b processing. *J.Immunol.* 161:3340-3346.

Figure 1

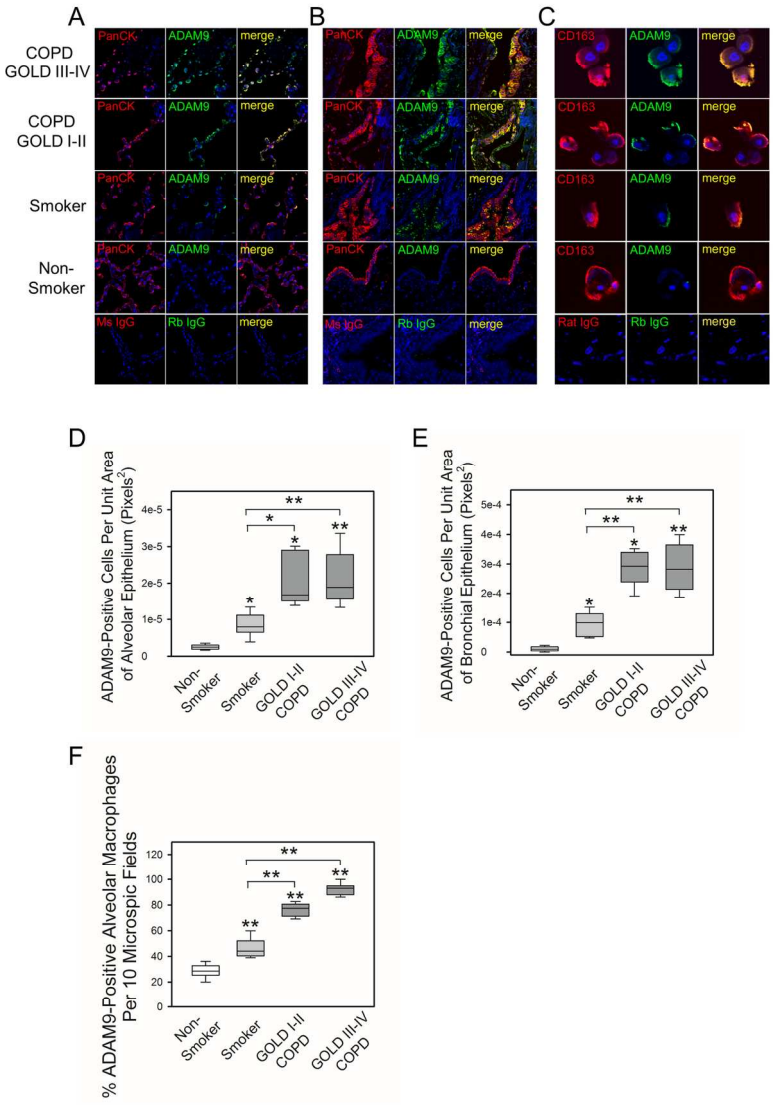

129x200mm (300 x 300 DPI)

AJRCCM Articles in Press. Published on 04-June-2018 as 10.1164/rccm.201711-2300OC

Figure 2

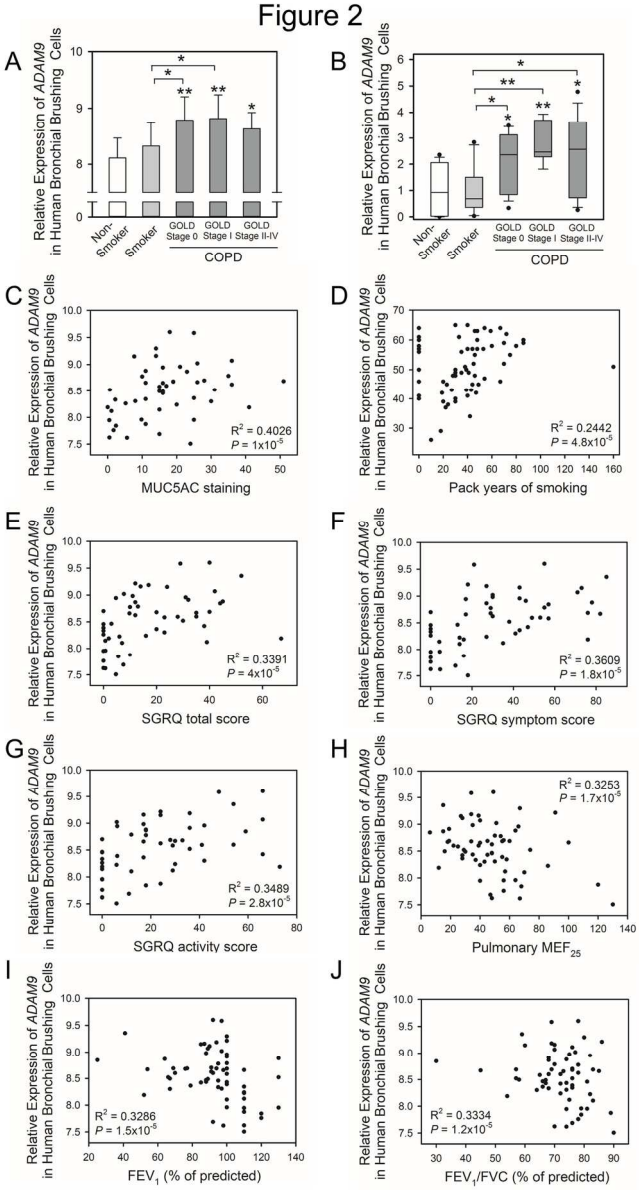

129x200mm (300 x 300 DPI)

Figure 3

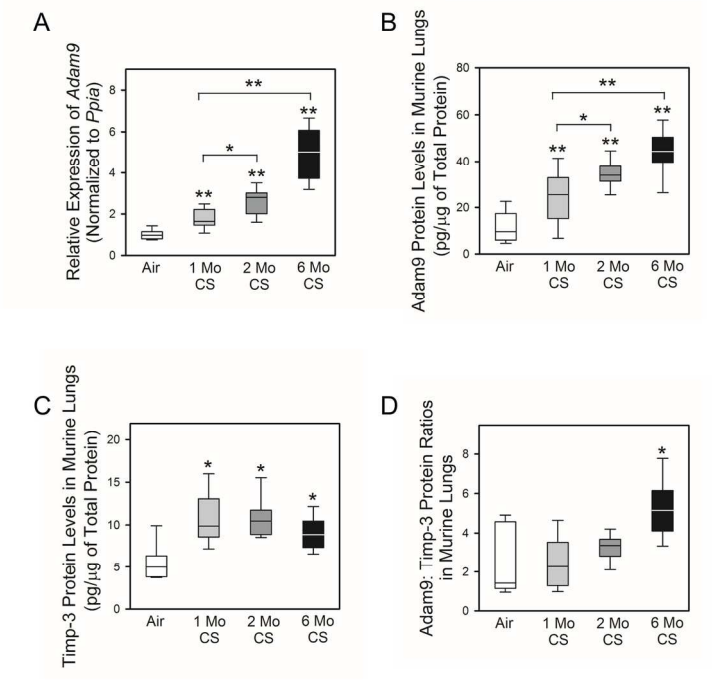

129x200mm (300 x 300 DPI)

AJRCCM Articles in Press. Published on 04-June-2018 as 10.1164/rccm.201711-2300OC

Figure 4

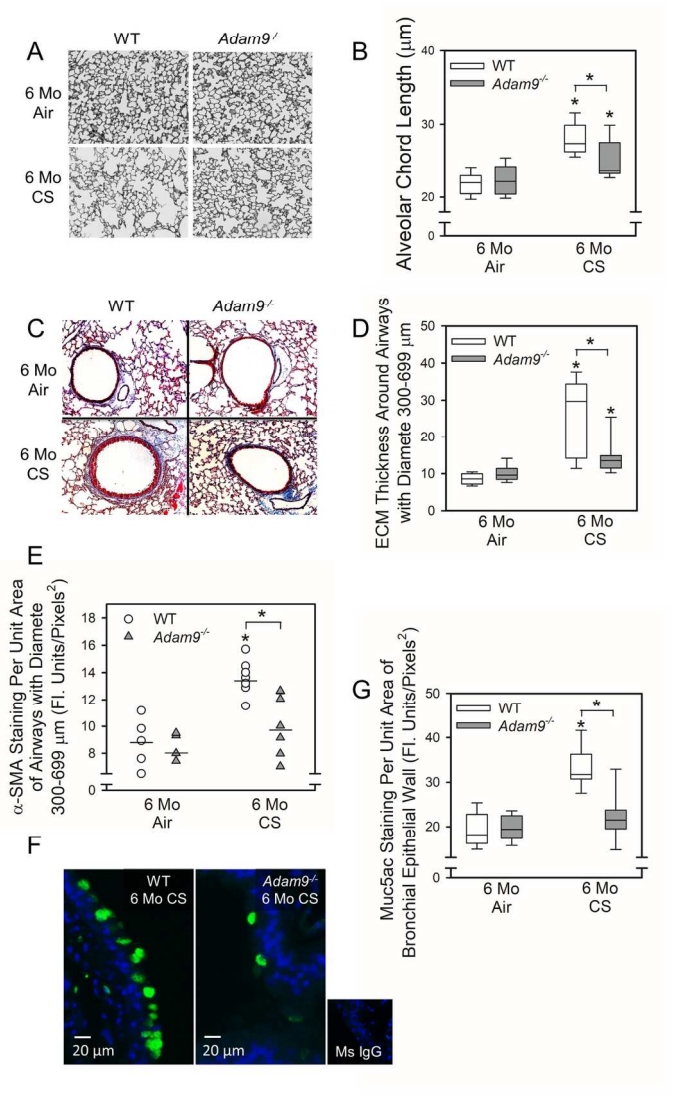

129x200mm (300 x 300 DPI)

Figure 5

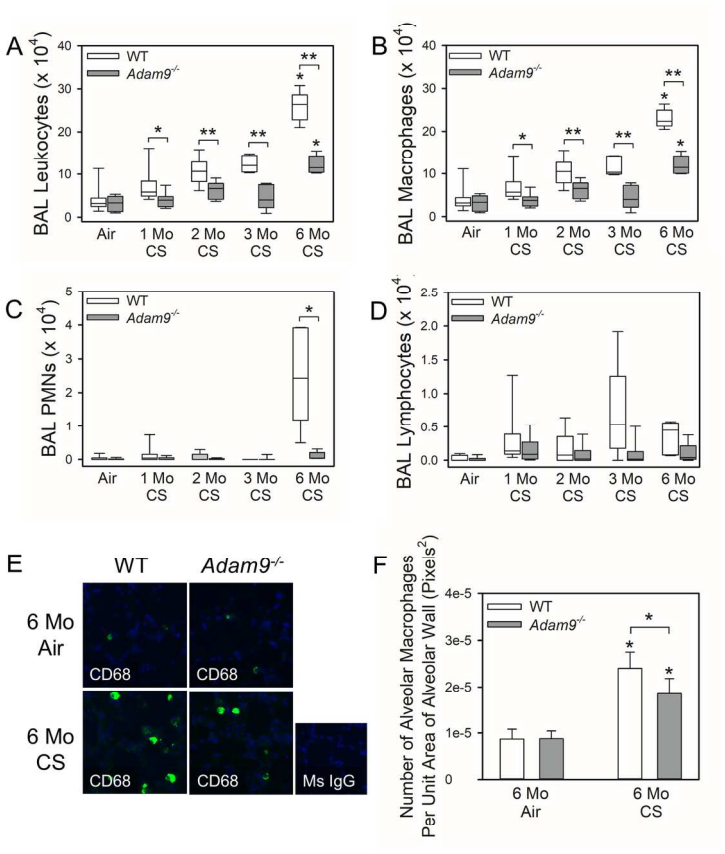

129x200mm (300 x 300 DPI)

AJRCCM Articles in Press. Published on 04-June-2018 as 10.1164/rccm.201711-2300OC

Figure 6

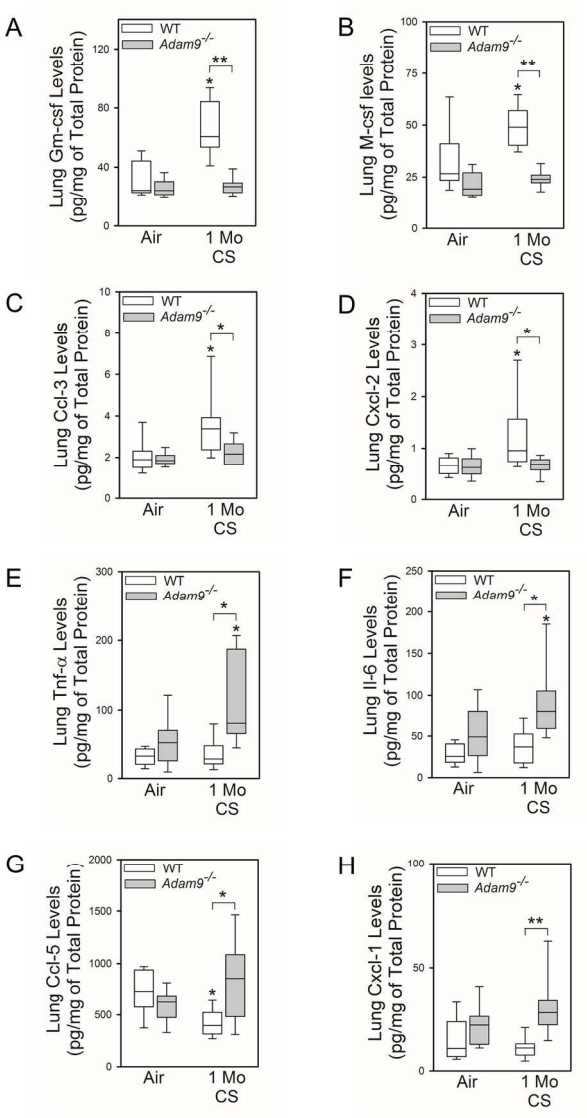

129x200mm (300 x 300 DPI)

Figure 7

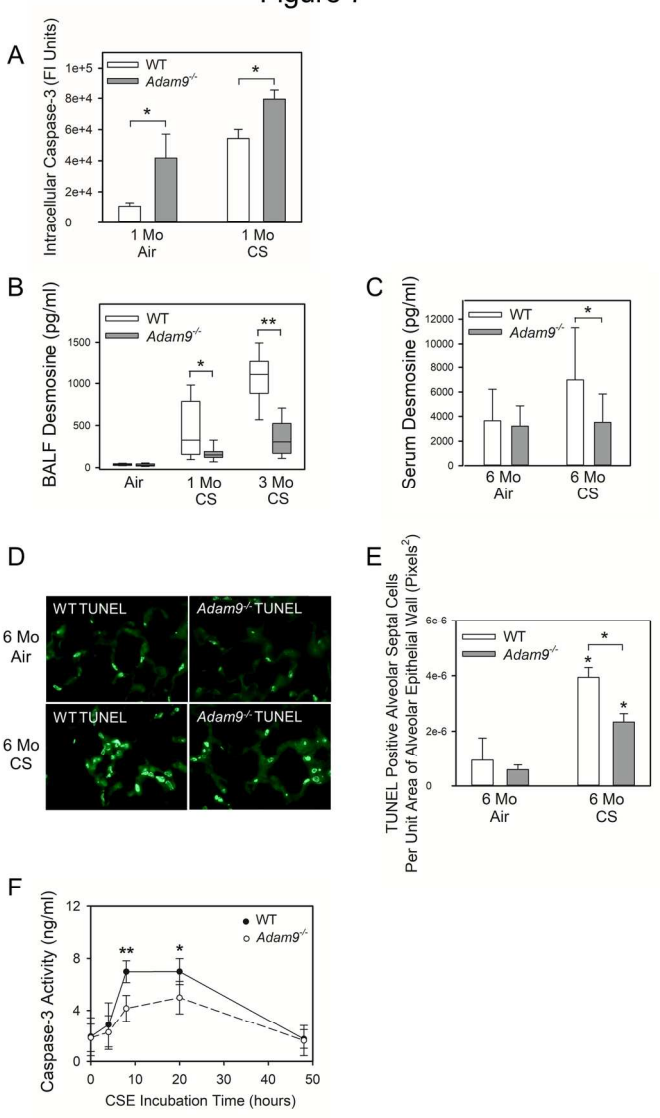

129x200mm (300 x 300 DPI)

AJRCCM Articles in Press. Published on 04-June-2018 as 10.1164/rccm.201711-2300OC

Figure 8

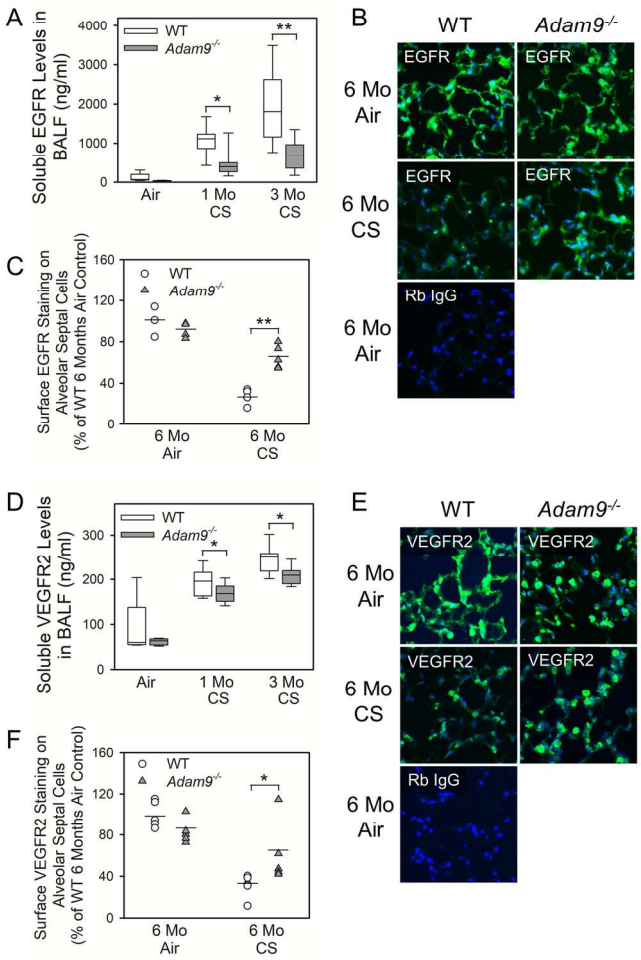

129x200mm (300 x 300 DPI)

Figure 9

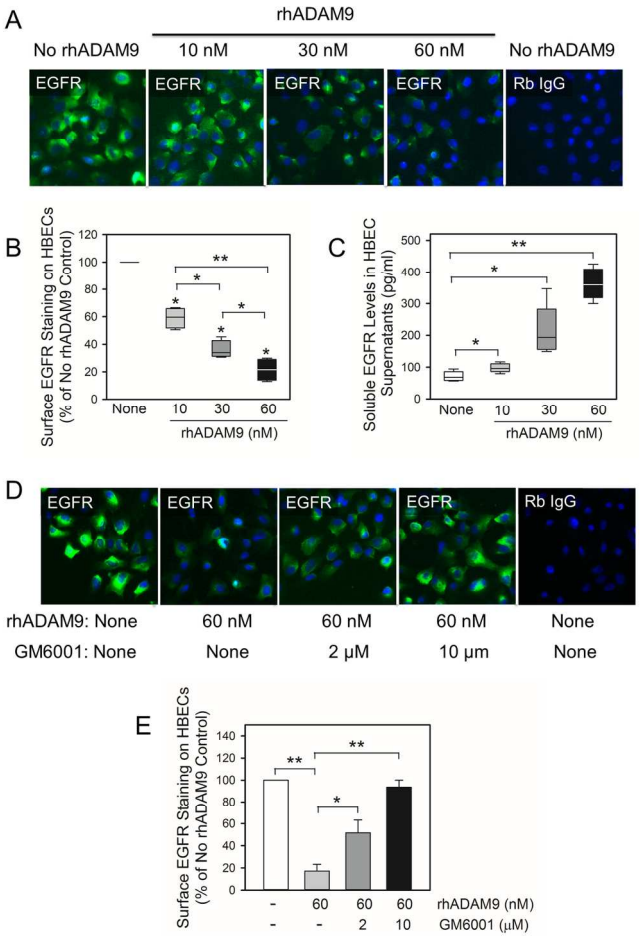

129x200mm (300 x 300 DPI)

AJRCCM Articles in Press. Published on 04-June-2018 as 10.1164/rccm.201711-2300OC

Figure 10

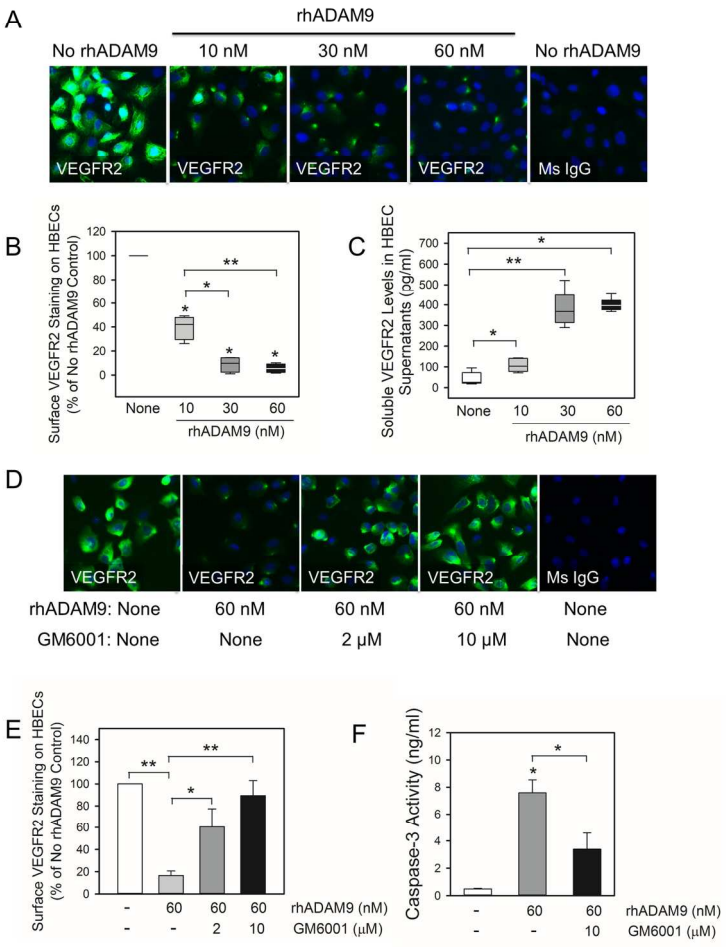

129x200mm (300 x 300 DPI)

Figure 11

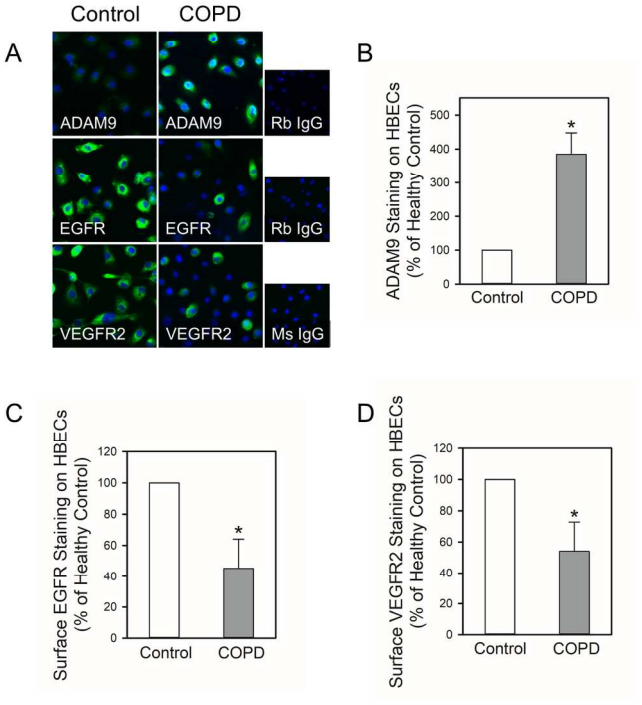

129x200mm (300 x 300 DPI)

AJRCCM Articles in Press. Published on 04-June-2018 as 10.1164/rccm.201711-2300OC

Figure 12

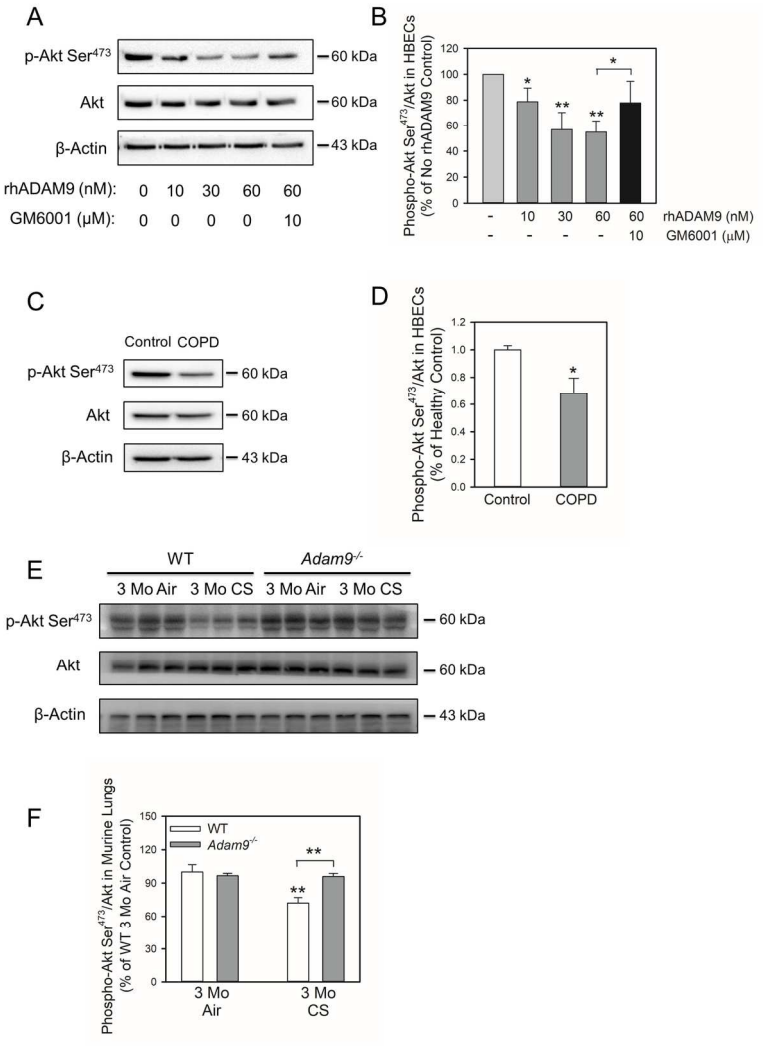

129x200mm (300 x 300 DPI)

Figure 13

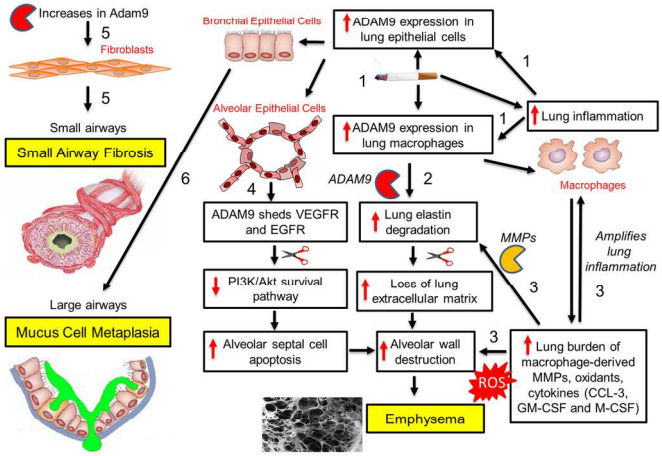

129x200mm (300 x 300 DPI)

AJRCCM Articles in Press. Published on 04-June-2018 as 10.1164/rccm.201711-2300OC

ONLINE SUPPLEMENT

MATERIALS AND METHODS

Materials: ELISA kits to measure human ADAM9, murine interleukin-6 (IL-6), murine Rantes (Ccl5), murine interleukin-10 (Il-10), murine interleukin-1 beta (Il-1β), murine Je (Ccl2), murine tumor necrosis factor-α (Tnf-α), and murine transforming growth factor-β (Tgf-β) were obtained from R & D Systems (Minneapolis, MN). ELISA kits to quantify murine granulocyte colony stimulating factor (G-csf), murine granulocyte macrophage colony-stimulating factor (Gm-csf), murine macrophage colony-stimulating factor (M-csf), murine macrophage inflammatory protein-1α (Mip-1α), murine Mip-2, and murine keratinocyte-derived chemokine (Kc) were purchased from Peprotech (Rocky Hill, NJ). The ELISA kit for quantifying murine Adam9 was obtained from CUSABIO (College Park, MD). Recombinant human ADAM9 was purchased from R&D System (Minneapolis, MN).

Human Subjects Studies

Four cohorts were studied: 1) a lung immunostaining cohort (Boston, USA); 2) bronchoscopy cohorts from which bronchoalveolar lavage fluid (BALF) samples (Manchester cohort, UK), and/or bronchial brushings (Southampton, UK and Manchester cohort, UK), or endobronchial biopsies (Southampton, UK) were obtained; 3) a sputum cohort (Manchester cohort, UK); and 4) a plasma cohort (Boston, USA and Manchester, UK). None of the human cohort studies was registered as a clinical trial. All studies of human subjects were approved by local institutional and regional review boards in the US and UK, respectively (Partners Healthcare Institutional Review Board #2014P001255; And the NRES Committee North West - Greater Manchester Central; reference code 06/Q1403/156; Southampton University and the General Hospitals ethics

committee: LREC 276/99 RHM MED 0657: Epithelial gene expression in COPD). The Southampton bronchial brushing samples yielded a whole genome microarray data set from which *ADAM9* gene expression data were extracted. The results of the study of gene expression in the epithelium have been reported previously (1). **Tables 1-2** and **E1-E3** and **E5** show the demographic and clinical data on the subjects studied.

Lung immunostaining cohort: We studied current or former smokers with COPD [Global Initiative for Obstructive Lung Disease (GOLD) stages I–IV]; smoker controls without COPD, and non-smokers. Current smokers were defined as active smokers at the time of the study or smokers that had stopped smoking less than 1 year prior to the study. The characteristics of all the subjects studied are described in **Table 1** and **Table E5**. Patients with a post-bronchodilator FEV_1/FVC ratios < 70% were considered to be COPD cases, and those with a post-bronchodilator FEV_1/FVC ratios $\geqslant$ 70% were considered to be controls for all of the cohorts listed below. Sections of lung were obtained from lung biopsies obtained from subjects with benign tumors or lobectomies for lung cancer (2 COPD cases, 2 smokers, and 1 non-smoker). In the lung cancer cases, lung tissue for study was taken > 10 cm from the cancer margin. ADAM9 staining was similar in the cancer and non-cancer cases in each group (data not shown). COPD lung tissue was also obtained from lung volume reduction surgeries, or from explanted lungs from COPD patients undergoing lung transplantation. Lung sections were provided by NHLBI-sponsored Lung Tissue Research Consortium (www.ltrcpublic.com), or the Department of Pathology at Brigham and Women's Hospital, Boston. None of the subjects studied had evidence of respiratory tract infection at the time of lung tissue sampling.

Double immunofluorescence staining of human lung sections for ADAM9: Immunofluorescence staining for ADAM9 was performed on formalin-fixed sections of human

AJRCCM Articles in Press. Published on 04-June-2018 as 10.1164/rccm.201711-2300OC

lung. The sections were incubated with a rabbit anti-ADAM9 IgG (Abcam, Cambridge, MA) or non-immune rabbit IgG, followed by Alexa 488-conjugated goat anti-rabbit $F(ab)_2$ (Invitrogen, Charlestown, MA). Sections were double stained with either: 1) rat anti-human CD163 IgG (Santa Cruz, Dallas, TX) followed by Alexa 546-conjugated goat anti-rat IgG; or 2) murine anti-human pancytokeratin (PanCK) (Sigma, St. Louis, MO) followed by Alexa 546-conjugated goat anti-murine IgG. All the secondary antibodies were obtained from Invitrogen (Charlestown, MA). Lung sections were also immuno-stained with appropriate isotype-matched non-immune control antibodies. Representative images were captured using a confocal microscope (Olympus corporations, Center Valley, PA). Images were captures using an epi-fluorescence microscope (Leica Biosystems, Buffalo Grove, IL). MetaMorph software (Molecular Devices, Sunnyvale, CA) was used to quantify immunostaining in epithelial cells which was normalized per unit of area of the alveolar or bronchial wall. To quantify ADAM9 expression in alveolar macrophages, the percentage of ADAM9-positively stained cells in 10 randomly acquired images per lung section was counted.

Triple immunofluorescence staining of human lung sections for ADAM9 and EGFR/ VEGFR2:

Triple immunofluorescence staining for pancytokeratin, ADAM9, and EGFR or VEGFR2 was performed on formalin-fixed sections of human lung. The sections were incubated with murine anti-human PanCK (Sigma, St. Louis, MO) followed by Alexa 546-conjugated goat anti-murine IgG (Invitrogen, Charlestown, MA). The sections were then stained with a goat anti-ADAM9 IgG (R & D Systems, Minneapolis, MN) or non-immune goat IgG, followed by Alexa 488-conjugated rabbit anti-goat $F(ab)_2$ (Invitrogen, Charlestown, MA). The sections were then stained with either: 1) rabbit anti-human EGFR IgG (Abcam, Cambridge, MA) followed by cyanine5 cross-adsorbed goat anti-rabbit IgG; or 2) rabbit anti-human VEGFR2 (Abcam, Cambridge, MA) followed by

cyanine5 cross-adsorbed goat anti-rabbit IgG. All of the secondary antibodies were obtained from Invitrogen (Charlestown, MA). Lung sections were also immuno-stained with appropriate isotype-matched primary non-immune control antibodies. Images were captured using a confocal microscope (Olympus corporations, Center Valley, PA).

ADAM9 steady state mRNA levels in primary human bronchial brushing cells: Airway brushing cells were obtained from clinically-stable COPD patients, non-smokers, and smokers without COPD (see **Table 2** for demographic and clinical data) by performing bronchoscopy and collecting bronchial brushings and endobronchial biopsies, as described previously (1). Total RNA was extracted from the brushed cells from COPD patients, non-smokers, and healthy smokers using TRIZOL® (Invitrogen, Paisley, UK) and stored in liquid nitrogen for subsequent microarray analysis of gene expression using Affymetrix GeneChip® arrays (Affymetrix, Santa Clara, California, USA). The RNA yield was determined spectrophotometrically and RNA integrity was evaluated by measuring the absorbance ratio (A260/A280) and running an aliquot on a 1% agarose gel. Ten μg of total RNA per sample was used to prepare the hybridization probes following the manufacturer's recommendations. Human Genome U133 GeneChip® arrays (Affymetrix, Santa Clara, CA, USA) were hybridized, washed, stained, and scanned according to the manufacturer's standard procedures (1).

A whole genome microarray data-set was generated from which *ADAM9* gene expression data were extracted. The results of the study of gene expression in the brushings samples have been reported previously (1). To validate the results of the microarray assay, real-time quantitative RT-PCR was performed on the samples (when there was sufficient quantify) using commercial Taqman probe and primer sets for ADAM9 and 18S ribosomal RNA as the housekeeping gene (Thermo Fischer Scientific Corp), and the comparative threshold method.

AJRCCM Articles in Press. Published on 04-June-2018 as 10.1164/rccm.201711-2300OC

Immunostaining of human endobronchial biopsies for MUC5AC: Endobronchial biopsies from the bronchoscopy population were embedded in glycol methacrylate resin and stained, as previously described (2). In brief, two micron sections were cut and stained immunohistochemically by the streptavidin biotin-peroxidase technique, with diamino benzidine visualisation, for MUC5AC. Immunoreactivity was quantified using computer-assisted image analysis as percentage area staining within the epithelium (3).

Soluble ADAM9 protein levels in plasma samples: Soluble ADAM9 protein levels were measured in plasma samples from never-smokers without COPD, smokers without COPD, and COPD patients (GOLD Stages I-II and III-IV) using commercially-available ELISAs (R&D Systems, Minneapolis, MN). See **Table E1** for the demographic and clinical data on the subjects studied.

Human BAL fluid (BALF) sample processing and quantification of soluble ADAM9 protein levels in BALF samples: Bronchoscopy was performed on 28 clinically-stable COPD patients and 7 smokers without COPD in the Manchester, UK cohort (**Table E2**). The bronchoscope was wedged in the bronchus and a maximum of 4 × 60 ml aliquots of pre-warmed sterile 0.9% NaCl solution were instilled into the right and/or left upper lobes. The aspirated BAL sample was stored on ice, and then filtered using a 100 μm filter (Becton Dickenson, UK). The filtrate was centrifuged (at 400 g for 10 min at 4°C) and the BALF sample was removed and stored in aliquots at -80ºC for further analysis. BALF ADAM9 levels were quantified using a commercially-available ELISA kit (R&D Systems, Minneapolis, MN).

Soluble ADAM9 protein sputum levels: Sputum was obtained from smokers without COPD, and clinically-stable COPD patients (GOLD Stages I-II and III-IV). See **Table E2** for clinical and demographic data on the subjects studied. Sputum was spontaneously expectorated into a sterile

pot. Following expectoration, sputum plugs were separated from saliva using sterile forceps, with one-third being taken for culture analysis when there was sufficient quantity. The remaining sputum was weighed and suspended in nine times the volume of standard isotonic phosphate-buffered saline (PBS). Glass beads were added to this suspension which was then homogenized by vortexing for 15 seconds, rocking for 15 min (IKA Vibrax VXR, Staufen, Germany), and additional vortexing was performed for 15 seconds. Aliquots of 500 µl were stored at -80ºC for subsequent batch processing. Sputum ADAM9 levels were quantified using a commercially-available ELISA kit (R&D Systems, Minneapolis, MN).

Animal Experiments

Animals: All studies conducted on mice were approved by the Institutional Care and Use Committee at Brigham and Women's Hospital. *Adam9*$^{-/-}$ mice in a pure C57BL/6 background were obtained from Carl Blobel (Hospital for Special Surgery, New York, NY). C57BL/6 wild-type (WT) mice were purchased from the Jackson Laboratory (Bar Harbor, ME). Mice were housed in a barrier facility under specific pathogen-free conditions, and their genotype was confirmed using PCR protocols performed on DNA extracted from tail biopsies.

CS exposures: Adult WT and *Adam9*$^{-/-}$ mice (males and females, aged 8-12 weeks old) were randomized to the experimental groups and exposed to air or mixed mainstream and side-stream CS from 3R4F Kentucky Research cigarettes for 2 h/day 6 days-a-week in Teague TE 10z chambers for 1-6 months (4).

Adam9 protein levels in murine lungs: Adam9 protein levels were measured in homogenates of lung samples from WT mice exposed to air or CS for 1 or 2 or 6 months using a commercially-available ELISA kit (CUSABIO, College Park, MD). Adam9 protein levels were

AJRCCM Articles in Press. Published on 04-June-2018 as 10.1164/rccm.201711-2300OC

normalized to total protein levels measured in the same samples using a commercial kit (Thermo-Fisher Scientific, Rockford, IL).

Adam9 steady state mRNA levels in murine lungs: *Adam9* steady-state mRNA levels were quantified in whole lung samples from WT mice exposed to air or CS for 1, 2 , or 6 months. Total RNA was isolated from lung samples using a SurePrep TrueTotal RNA Purification Kit (Fisher Scientific, Fair Lawn, NJ), following the manufacturer's instructions, and 1 μg of RNA was reverse transcribed into cDNA using High-Capacity cDNA Reverse Transcription Kit (Thermo Fisher Scientific, Carlsbad, CA). SYBR green-based real-time RT-PCR was used to measure *Adam9* gene expression using primers from Invitrogen (Charlestown, MA) Ppia and β-actin as the housekeeping genes (see **Table E6** for primer sequences), the comparative threshold method, and an AriaMx Real-time PCR machine (Agilent technologies, Santa Clara, CA).

Measurements of emphysema and small airway fibrosis: WT and *Adam9*$^{-/-}$ mice were exposed to air or CS for 6 months, and serum samples were obtained post-euthanasia *via* right ventricular puncture. Lungs were inflated to 25 cm H_2O pressure and fixed in 10% buffered formalin. Airspace size was measured as alveolar chord length on Gill's-stained and inflated lung sections from mice exposed to air or CS for 6 months using morphometric methods (4). Fibrosis around small airways having a mean diameter of 300-699 microns was quantified on Masson's Trichrome-stained and inflated lung sections from mice exposed to air or CS for 6 months using morphometric methods (4).

Immunofluorescence staining of murine lung sections for α-smooth muscle actin (α-SMA): WT and *Adam9*$^{-/-}$ mice were exposed to air or CS for 6 months. Lungs were inflated to 25 cm H_2O pressure and fixed in 10% buffered formalin. The lung sections were deparaffinized, and antigen

retrieval was performed by heating the slides in a microwave in 10 mM citrate buffer (pH 6.0) for 10 min. The sections were incubated at 4°C overnight with a murine IgG to α-SMA (diluted 1:20, Sigma, St. Louis, MO) or non-immune murine IgG at the same concentration. After washing the lung sections with PBS, the sections were incubated for 1 h at 37°C with Alexa 488-conjugated rabbit anti-murine $F(ab')_2$. Images were captured using a digital camera. MetaMorph software (Molecular Devices, Sunnyvale, CA) was used to quantify immunostaining around small airways having a mean diameter of 300-699 microns which was normalized per unit of area of the bronchial wall.

Immunofluorescence staining of murine lung sections for Muc5ac: To identify the Muc5ac-positive cells in bronchial epithelial cells, immunofluorescence staining was performed on lung sections from mice exposed to air versus CS for 6 months. Briefly, the lung sections were deparaffinized, and antigen retrieval was performed by heating the slides in a microwave in 10 mM citrate buffer (pH 6.0) for 10 min. The sections were incubated at 4°C overnight with a murine IgG to Muc5ac (diluted 1:20; ThermoFisher Scientific, Waltham, MA) or non-immune murine IgG applied at the same concentration. After washing the lung sections with PBS, the sections were incubated for 1 h at 37°C with Alexa 488-conjugated rabbit anti-murine $F(ab')_2$ or Alexa 546-conjugated rabbit anti-murine $F(ab')_2$ (Invitrogen, Carlsbad, CA). Images were captured using a digital camera. The number of Muc5ac-positive cells was counted and normalized to the bronchial epithelial cell area measured using Metamorph (Molecular Devices, Sunnyvale, CA).

Lung inflammation: All leukocytes, macrophages, PMNs, and lymphocytes were counted in BAL samples from WT and *Adam9*$^{-/-}$ mice exposed to air or CS for 1-6 months (5). In other cohorts of WT and *Adam9*$^{-/-}$ mice exposed to air or CS for 1 month, lungs were removed, and homogenized in lysis buffer (PBS containing 0.5% Triton, 1 mM phenylmethanesulfonylfluoride

AJRCCM Articles in Press. Published on 04-June-2018 as 10.1164/rccm.201711-2300OC

(PMSF), 1 mM 1,10 phenanthroline, and 1% Sigma Mammalian Protease Inhibitor Cocktail). Pro- and anti-inflammatory mediators were measured in homogenates of lung samples using commercially-available ELISAs, and lung levels of mediators were normalized to lung total protein levels.

Immunofluorescence staining of murine lung sections for a marker of macrophages: Lung sections from WT and *Adam9*$^{-/-}$ mice that had been exposed to air or CS for 6 months were immunostained for a marker of macrophages (CD68). Briefly, the lung sections were de-paraffinized, and antigen retrieval was performed by heating the slides in a microwave oven in 10 mM citrate buffer (pH 6.0) for 10 min. The sections were incubated at 4°C for 18 h with a murine polyclonal IgG to CD68 diluted 1:50 (Abcam, Cambridge, MA) or a non-immune murine IgG added at the same concentration. After washing the lung sections with PBS, the sections were incubated for 1 h at 37°C with Alexa 488-conjugated goat anti-murine $F(ab')_2$ (Invitrogen, Carlsbad, CA). The slides were washed in PBS, and nuclei were counterstained with 4',-6-diamidino-2-phenylindole (DAPI). Images of the stained lung sections were captured using a digital camera. The number of CD68-positive cells was counted and normalized to the alveolar area measured using Metamorph (Molecular Devices, Sunnyvale, CA).

Activity assay of recombinant human ADAM9 protein (rhADAM9): To confirm that the rhADAM9 preparation (R&D System, Minneapolis, MN) was active, 20 nM ADAM9 was incubated at 37°C in duplicate for up to 18 h with 10 μM Fluorogenic Substrate III (R&D System, Minneapolis, MN), a sensitive substrate for ADAM9 (6). Cleavage of the substrate was measured using fluorimetry (Ex λ 320nm and Em λ 504nm) exactly as described previously (6).

Incubation of active human recombinant ADAM9 (rhADAM9) with cytokines and chemokines: To test whether the active metalloproteinase domain of ADAM9 cleaves or degrades cytokines or

chemokines *in vitro*, cytokines that were elevated in the lungs of CS-exposed *Adam9*$^{-/-}$ versus CS-exposed WT mice were incubated with and without active rhADAM9. Preliminary experiments optimized the concentrations of mediators that were needed to produce signals on silver-stained Tris-tricine gels. Human interleukin (IL)-6 (900 nM), CCL5 (3200 nM), IL-8 (2750 nM), or TNF-α (1149 nM) were incubated in a total volume of 20 µL of assay buffer (25 mM Tris containing 2.5 µM $ZnCl_2$ and 0.05% Briji-35; pH 9.0) with or without active 0.3 µM rhADAM9 either with or without 1 mM 1,10-phenanthroline (a non-selective inhibitor of metalloproteinases that inhibits ADAMs) for 18 h at 37^{o}C temperature. Reaction products were separated on Tris-tricine gels and visualized using a silver staining kit (Thermo Fisher Scientific).

Degradation of lung elastin by Adam9: WT versus *Adam9*$^{-/-}$ mice were exposed to air or CS for 1 or 3 months. Serum was collected post-euthanasia *via* right ventricular puncture, and the lungs were lavaged with 750 µl of PBS. Desmosine (a marker of elastin degradation) was quantified in cell-free BALF and serum samples using a commercially-available ELISA kit (CUSBIO, College Park, MD).

Apoptosis of alveolar macrophages: To quantify alveolar macrophages apoptosis *in vivo*, WT and *Adam9*$^{-/-}$ mice were exposed to air or CS for 1 month. Alveolar macrophages were isolated from the lungs using BAL, and immediately fixed with PBS containing 3% paraformaldehyde and 0.25% glutaraldehyde (pH 7.4) for 3 min at 4^{o}C. To obtain sufficient cells for analysis in each of 3 separate experiments, BAL macrophages were pooled from 4 air-exposed WT mice, 5 air-exposed *Adam9*$^{-/-}$ mice, 3 CS-exposed WT mice, and 3-4 CS-exposed *Adam9*$^{-/-}$ mice. The pooled cells were permeabilized by incubating them in 100% ice-cold methanol for 20 min at 4 ^{o}C. Intracellular levels of active caspase-3 were measured by blocking the cells with PBS containing 1% albumin and 5% normal goat serum, and then incubating the cells with rabbit

AJRCCM Articles in Press. Published on 04-June-2018 as 10.1164/rccm.201711-2300OC

anti-cleaved caspase-3 IgG (Cell Signaling, Danvers, MA) diluted 1:50 or the same concentration of non-immune rabbit IgG followed by Alexa-488-conjugated goat anti-rabbit $F(ab)_2$. Images of the immunostained cells were acquired using a Leica microscope and a digital camera. Intracellular immunofluorescence staining (in arbitrary fluorescence units) was quantified in 300 cells per group using MetaMorph software (Molecular Devices, LLC) (10). Data were corrected for non-specific staining in the presence of the non-immune control antibody as described previously (10).

Alveolar septal cell death: To quantify alveolar septal cell death in murine lungs, we double immune-stained fixed and inflated lung sections from WT and *Adam9*$^{-/-}$ mice exposed to air or CS for 6 months using an Apoalert DNA Fragmentation Detection Kit (Clontech, Mountain View, CA) to stain injured cells green, followed by a murine anti-pan-cytokeratin IgG (Abcam), followed by Alexa 546-conjugated goat anti-murine IgG (H+L) (Invitrogen, Carlsbad, CA) to label epithelial cells red. Images of the stained sections were captured using an epifluorescence microscope (Leica Biosystems, Buffalo Grove, IL). The number of TUNEL-positive alveolar septal cells was counted and normalized to the area of the alveolar walls which was measured using MetaMorph software (Molecular Devices, Sunnyvale, CA).

CS extract (CSE): CSE was prepared by allowing smoke from two 1R3F cigarettes (University of Kentucky, Lexington, KY) to bubble through 10 ml of DMEM medium to yield a 100% CSE solution. CSE was filtered and immediately added to cell cultures to yield the stated final concentration of CSE for each experiment. Preliminary dose-response and time-course experiments confirmed that the concentration of CSE chosen and the time points studied were optimal for inducing apoptosis for each cell type studied.

Intracellular active caspase-3 levels in CSE-treated lung epithelial cells: Murine type-II alveolar epithelial cells were isolated from naïve WT and *Adam9*$^{-/-}$ mice as described previously (7). Monolayers of the cells were cultured on tissue culture dishes (Corning, New York, NY) that had been coated with Matrigel and type I collagen (Corning, New York, NY). The purity of these cells (> 95%) was confirmed by immunostaining the cells for pulmonary-associated surfactant protein-C (SP-C). After culturing the cells for 7 days in BEBM medium (Lonza, Allendale, NJ) containing BEGM growth supplement (Lonza, Allendale, NJ), the cells were incubated with or without 7.5% cigarette smoke extract (CSE) prepared as described previously (5). At intervals up to 48 h, the cells were lyzed in caspase-3 lysis buffer, and intracellular levels of active caspase-3 were measured using a fluorogenic substrate that is specific for caspase-3 (BD Biosciences, Franklin Lakes, NJ), standards of known concentrations of recombinant caspase-3 (R&D, Minneapolis, MN), and fluorimetry (Ex 400 λ and Em λ 490) as described previously (8).

Intracellular active caspase-3 levels in CSE-treated bone marrow-derived macrophages (BMDMs): BMDMs were isolated from naïve WT and *Adam9*$^{-/-}$ mice as described previously (9). BMDMs were cultured in L929-conditioned medium for 7 days, and then the media were changed to normal complete medium. Cells were incubated with or without 20% CSE, at intervals up to 48 h, cells were lyzed in caspase-3 lysis buffer, and intracellular levels of active caspase-3 were measured (8).

Shedding of epidermal growth factor receptor (EGFR) and vascular endothelial growth factor receptor-2 (VEGFR2) in murine lungs: WT and *Adam9*$^{-/-}$ mice were exposed to air or CS for 1, 3, or 6 months. BAL was performed (using 750 µl of PBS/mouse), and cell-free BALF was frozen in aliquots to -80°C. Lungs were inflated to 25 cm H_2O pressure and fixed in 10% buffered

AJRCCM Articles in Press. Published on 04-June-2018 as 10.1164/rccm.201711-2300OC

formalin. Levels of soluble EGFR and soluble VEGFR2 were measured in cell-free BALF and serum samples using commercially-available ELISA kits (R&D Systems, Minneapolis, MN and MyBiosource, San Diego, CA, respectively).

Residual EGFR and VEGFR2 expressed on alveolar epithelial cell surfaces were measured in the formalin-fixed inflated lung sections using immunostaining. Briefly, lung sections were incubated with rabbit anti-EGFR IgG (Santa Cruz, Dallas, TX), rabbit anti-VEGFR2 IgG (Abcam, Cambridge, MA), or non-immune rabbit IgG (Dako, Santa Clara, CA), followed by Alexa 488-conjugated goat anti-rabbit anti-goat $F(ab)_2$ (Invitrogen, Charlestown, MA). Images were captured using a high-speed 5 megapixel microscope camera (AxioCam, Zeiss, Oberkochen, Germany), a N-Achroplan 20×/0.45 objective lens (Zeiss, Oberkochen, Germany), and a software package (AxioVision, Zeiss, Oberkochen, Germany). MetaMorph software (Molecular Devices, Sunnyvale, CA) was used to measure the mean cell-associated EGFR or VEGFR2 fluorescence (in arbitrary fluorescence units) as described previously (10).

Shedding of epidermal growth factor receptor (EGFR) and vascular endothelial growth factor receptor-2 (VEGFR2) from human bronchial epithelial cell (HBECs) surfaces by rhADAM9: To determine whether ADAM9 sheds EGFR and/or VEGFR2 from lung epithelial cells, primary HBECs (Lonza, Allendale, NJ) were cultured in 8-well chamber slides (Corning, New York, NY) in BEBM medium (Lonza, Allendale, NJ) containing BEGM growth supplement (Lonza, Allendale, NJ) until they were confluent. The HBECs were then incubated with or without up to 60 nM active rhADAM9 for 4 h at 37ºC in assay buffer (25 mM Tris containing 2.5 µM $ZnCl_2$; pH 7.4) in the presence or absence of 2 µM or 10 µM GM6001,a non-selective metalloproteinase inhibitor (Sigma, St. Louis, MO). Soluble EGFR and soluble VEGFR2 levels were measured in

the cell-free supernatants using commercially-available ELISA kits (Aviscera Bioscience, Santa Clara, CA and R&D System, Minneapolis, MN, respectively).

The HBECs were fixed and residual EGFR and VEGFR2 expressed on HBEC surfaces were measured using immuno-staining. Briefly, the slides were incubated with rabbit anti-human EGFR IgG (Abcam, Cambridge, MA), murine anti-human VEGFR2 IgG (OriGene Technologies, Rockville, MD), or non-immune rabbit IgG (Dako, Santa Clara, CA), or non-immune murine IgG (Dako, Santa Clara, CA) followed by either Alexa 488-conjugated goat anti-rabbit $F(ab)_2$ (Invitrogen, Charlestown, MA) or Alexa 488-conjugated goat anti-murine $F(ab)_2$ (Invitrogen, Charlestown, MA). Images were captured using a high-speed 5 megapixel microscope camera (AxioCam, Zeiss, Oberkochen, Germany), a N-Achroplan 20×/0.45 objective lens (Zeiss, Oberkochen, Germany), and a software package (AxioVision, Zeiss, Oberkochen, Germany). MetaMorph software (Molecular Devices, Sunnyvale, CA) was used to measure cell-associated EGFR or VEGFR2 fluorescence (in arbitrary fluorescence units) as described previously (10).

ADAM9 induces apoptosis in primary HBECs: To determine ADAM9 promotes apoptosis of HBECs, primary HBECs (Lonza, Allendale, NJ) were cultured in 6-well culture plate (Corning, New York, NY) in bronchial epithelial basal medium (BEBM; Lonza, Allendale, NJ) containing BEGM growth supplements (Lonza, Allendale, NJ) until they were confluent. The HBECs were incubated with or without up to 60 nM active rhADAM9 at 37^{o}C for 4 h in the presence or absence of 10 μM GM6001 (a non-selective metalloproteinase inhibitor that inhibits ADAM9; Sigma, St. Louis, MO). HBECs were lyzed in caspase-3 lysis buffer, and intracellular levels of active caspase-3 were measured using a fluorogenic substrate that is specific for caspase-3 (BD Biosciences, Franklin Lakes, NJ), standards of known concentrations of recombinant caspase-3

AJRCCM Articles in Press. Published on 04-June-2018 as 10.1164/rccm.201711-2300OC

(R&D, Minneapolis, MN), and fluorimetry (Ex 400 λ and Em λ 490) exactly as described previously (8).

ADAM9, EGFR, and VEGFR2 staining in primary HBECs derived from controls and COPD patients: Primary HBECs from COPD patients and controls without COPD were obtained from a commercial source (Lonza, Allendale, NJ). HBECs were cultured on 8-well chamber slides (Corning, New York, NY) in BEBM medium (Lonza, Allendale, NJ) containing BEGM growth supplement (Lonza, Allendale, NJ) until they were confluent. The HBECs were fixed, and levels of ADAM9, EGFR, and VEGFR2 that expressed on HBEC surfaces were measured using immuno-staining. Briefly, the cells were first incubated at 4^{o}C with PBS containing 1% albumin and 50 µg/ml goat IgG to block non-specific binding of antibodies. Cells in different wells in the chamber-slides were then incubated at 4^{o}C with either rabbit anti-human ADAM9 (Abcam, Cambridge, MA), rabbit anti-human EGFR IgG (Abcam, Cambridge, MA), murine anti-human VEGFR2 IgG (OriGene Technologies, Rockville, MD), non-immune rabbit IgG (Dako, Santa Clara, CA), or non-immune murine IgG (Dako, Santa Clara, CA). Cells were washed twice in PBS and then incubated with either Alexa 488-conjugated goat anti-rabbit F(ab)$_2$ (Invitrogen, Charlestown, MA) or Alexa 488-conjugated goat anti-murine F(ab)$_2$ (Invitrogen, Charlestown, MA). Images were captured using a high-speed 5 megapixel microscope camera (AxioCam, Zeiss, Oberkochen, Germany), a N-Achroplan 20×/0.45 objective lens (Zeiss, Oberkochen, Germany), and a software package (AxioVision, Zeiss, Oberkochen, Germany). MetaMorph software (Molecular Devices, Sunnyvale, CA) was used to measure cell-associated ADAM9, EGFR, or VEGFR2 fluorescence (in arbitrary fluorescence units) corrected for non-specific staining as described previously (10).

ADAM9 reduces activation (phosphorylation) of Akt: To determine whether ADAM9 alters the phosphorylation status of the pro-survival phosphatidylinositol 3 kinase (PI3K)-Akt pathway, primary HBECs from subjects without COPD (Lonza, Allendale, NJ) were cultured on 6-well culture plate (Corning, New York, NY) in BEBM medium (Lonza, Allendale, NJ) containing BEGM growth supplement (Lonza, Allendale, NJ) until they were confluent. The HBECs were incubated with or without up to 60 nM active rhADAM9 at 37^{o}C for 4 h in the presence and absence of 10 μM GM6001 (a non-selective metalloproteinase inhibitor that inhibits ADAMs; Sigma, St. Louis, MO). Cells were lyzed in radioimmunoprecipitation assay (RIPA) buffer containing 1 mM phenylmethanesulfonylfluoride, 1 mM 1,10 phenanthroline, 1% Sigma Mammalian Protease Inhibitor Cocktail, and PhosSTOP (Sigma, St. Louis, MO). Western Blot analysis for total Akt and phospho-Akt (Ser^{473}) was performed as described previously (11).

For *in vivo* experiment, WT and *Adam9*$^{-/-}$ mice exposed to air or CS for 3 months, lungs were removed, and homogenized in RIPA buffer containing 1 mM phenylmethanesulfonylfluoride, 1 mM 1,10 phenanthroline, 1% Sigma Mammalian Protease Inhibitor Cocktail and PhosSTOP (Sigma, St. Louis, MO). The total protein concentration was determined using a BCA protein assay kit (Thermo-Fisher Scientific, Rockford, IL). Protein lysates were separated on 12% SDS-PAGE gels, transferred to PVDF membranes, and then incubated with rabbit anti-Akt IgG (Cell Signaling Technology, Danvers, MA), rabbit anti-Ser^{473} phospho-Akt IgG (Cell Signaling Technology, Danvers, MA), or rabbit anti-β-actin IgG (Santa Cruz, Dallas, TX). Membranes were then incubated with goat anti-rabbit IgG-conjugated to horse raddish peroxidase (Bio-Rad, Hercules, CA), and signals were developed using a chemiluminescence kit. Western blot images were captured and analyzed using a Chemidoc (Bio-Rad, Hercules, CA).

AJRCCM Articles in Press. Published on 04-June-2018 as 10.1164/rccm.201711-2300OC

Phospho-Akt levels in HBECs derived from controls and COPD patients: Primary HBECs from control subjects without COPD (n = 3) and COPD patients (n = 3) were obtained from a commercial source (Lonza, Allendale, NJ). The cells were plated on 6-well culture plate (Corning, New York, NY) in BEBM medium (Lonza, Allendale, NJ) containing BEGM growth supplements (Lonza, Allendale, NJ), and cultured until confluent. Cells were lyzed in radioimmunoprecipitation assay (RIPA) buffer containing 1 mM phenylmethanesulfonylfluoride, 1 mM 1,10 phenanthroline, 1% Sigma Mammalian Protease Inhibitor Cocktail, and PhosSTOP (Sigma, St. Louis, MO). Western Blot analysis for total Akt and phospho-Akt (Ser^{473}) was performed as described previously (11).

Statistical analyses: Non-parametic data are presented as box-plots showing medians and 25^{th} and 75^{th} percentiles and whiskers showing 10^{th} and 90^{th} percentiles or scatter plots. Parametric data are presented as means ± SD or SEM.

Human studies were analyzed using R v3.4 for Windows. Non-parametic data were analyzed using a One-Way ANOVA followed by Dunnett corrections for multiple comparisons. For correlation analyses, a multivariate regression model with ADAM9 positively stained cells per unit area of alveolar epithelium, or bronchial epithelium, or the number of ADAM9 positively stained macrophages per 10 micropic fields as the dependent variable, to identify the clinical parameters for which to adjust ADAM9 staining in each case. For group comparisons of ADAM9 gene expression in bronchial brushings, data were analyzed using a Bayesian regression model with informative normal priors on the correcting variables (age and pack-year smoking history). A more restrictive prior distribution was set on age as the multivariate analysis showed that age

correlated weakly with *ADAM9* gene expression. Contrasts were performed against the relevant group, and results are reported as the posterior probability of no effect.

Murine data were analyzed using SigmaPlot™ (Systat Software, San Jose, CA). Parametric data were analyzed with One-Way ANOVAs followed by pair-wise comparisons using Student's t-tests and Bonferroni corrections. Non-parametric data were analyzed with Kruskal-Wallis One-Way ANOVAs followed by pair-wise comparisons using Mann-Whitney U-tests with Bonferroni corrections.

AJRCCM Articles in Press. Published on 04-June-2018 as 10.1164/rccm.201711-2300OC

Table E1: Demographic and clinical characteristics of the bronchoscopy (bronchial brushings) cohort studied in real-time quantitative PCR analysis of *ADAM9* gene expression.

Characteristics	Non-smokers* (N = 14)	Smokers* (N = 15)	COPD GOLD stage 0* (N = 17)	COPD GOLD stage I* (N = 8)	COPD GOLD stages II-IV* (N = 13)	*P* value‡
Number of males (%)	9 (64)	7 (47)	6 (35)	6 (75)	9 (69)	***NS***
Age (years)	50 ± 9	45 ± 10	50 ± 7	58 ± 6	54 ± 7	***NS***‡
Pack-yrs. of smoking	0	33 (10-59)	46 (19-160)	38 (0-53)	60 (30-86)	***P* < 0.001**†
Number of current smokers (%)	0 (0)	15 (100)	17 (100)	6 (75)	11 (85)	***P* < 0.001**¶
FEV_1 (% of predicted)	110 (84-121)	110 (88-130)	97 (76-130)	92 (85-100)	61 (25-79)	***P* < 0.001**§
FEV_1/FVC (% of predicted)	78 (70-86)	80 (72-90)	76 (70-81)	68 (60-70)	59 (30-69)	***P* < 0.001**§§

The table shows the demographic and clinical characteristics of the COPD patients, smokers without COPD, and never-smokers that underwent a bronchoscopy to obtain bronchial brushings for analysis of *ADAM9* steady-state mRNA levels in the brushing cells and endobronchial biopsies

to quantify MUC5AC staining in bronchial epithelial cells. Data are presented as median (interquartile range) for non-parametric data or mean ± SD for parametric data.

* Subjects were classified as non-smokers, smokers without COPD, and COPD patients. Only those smokers with normal lung function and a high-resolution computed tomographic thoracic scan showing no evidence of emphysema were included in the smoker group. The COPD subjects were further classified according to the criteria of the Global Initiative for Obstructive Lung Disease (GOLD) into three groups: GOLD stage 0 COPD [having a chronic cough and sputum production but normal spirometry (n = 17)]; GOLD stage I COPD, with or without cough and sputum production and with $FEV_1 \geq 80\%$ of predicted but $FEV_1/FVC < 70\%$ (n = 8), and GOLD stage II-IV COPD, with or without cough and sputum production but with FEV_1 between 25% and 79% of predicted and $FEV_1/FVC < 70\%$ (n = 13). The subject groups were matched for age.

‡ Categorical variables were analyzed with Chi-Square tests. Statistical analyses included One-Way ANOVA tests for continuous variables (age, FEV_1 % predicted, FEV_1/FCV, and pack/years) followed by pair-wise comparisons using Student's t-tests (for parametric data) or Mann-Whitney U tests (for non-parametric data).

† The pack/year smoking histories of the COPD GOLD stages II-IV, GOLD stage I, GOLD stage 0 groups and the smoker group were significantly higher than that of the non-smokers by design. The smokers and GOLD 0 and GOLD I COPD patients were matched for pack-year smoking histories. The GOLD stage II-IV COPD patients had a significantly greater pack-year smoking history than the smoker group.

AJRCCM Articles in Press. Published on 04-June-2018 as 10.1164/rccm.201711-2300OC

¶The proportion of current smokers in the smoker group and COPD GOLD stage 0, I, and II-IV group was significantly higher than that of the non-smoker group by design. The proportion of current smokers was similar in the smoker group, and COPD GOLD stages 0, I, and II-IV groups.

§ The FEV_1 of the COPD GOLD stages II-IV group was significantly lower than that of the smoker and non-smoker groups ($P < 0.001$ for both comparisons). The FEV_1 of the COPD GOLD stage I group was also significantly lower than that of the smoker and non-smoker groups ($P < 0.05$ for both comparisons). The FEV_1 of the COPD GOLD stage 0 group was significantly lower than that of the non-smoker group ($P < 0.05$), but not significantly different from that of the smoker group ($P = 0.055$).

§§The FEV_1/FVC ratio of the COPD GOLD stages II-IV group was significantly lower than that of the smoker and non-smoker groups ($P < 0.001$ for both comparisons). The FEV_1/FVC ratio of the COPD GOLD stage I group was significantly lower than that of the smoker and non-smoker groups ($P < 0.001$ for both comparisons). The FEV_1/FVC ratio of the COPD GOLD stage 0 group was significantly lower than that of the smoker group ($P < 0.05$), but was not significantly different from that of the non-smoker group ($P = 0.206$).

NS: Not significant.

Table E2: Demographic and clinical characteristics of the subjects in the plasma cohort.

Characteristics of the plasma cohort	Non-smokers* (N = 28)	Smokers* (N = 42)	COPD GOLD stages I-II (N = 46)	COPD GOLD stages III-IV (N = 55)	*P* value‡
Males (%)	19 (68)	18 (43)	32 (69)	36 (65)	***NS***
Age (yrs.)	68 (46-77)	62 (43-75)	66 (53-83)	69 (37-82)	***NS***‡
Pack-yrs. of smoking	0	31 (12-96)	46 (16-160)	63 (21-160)	***P* < 0.001**‖
Current smokers (%)	0	9 (21)	17 (36)	10 (18)	***P* = 0.002**¶
FEV_1 (% of predicted)	92 (80-141)	93 (80-119)	59 (50-99)	38 (10-49.7)	***P* < 0.001**§
FEV_1/FVC (% of predicted)†	76 (70-86)	77 (71-87.8)	49 (37.8-67)	38 (24.7-59)	***P* < 0.001**§§

The table shows the demographic and clinical characteristics of the COPD patients, smokers without COPD, and non-smokers included in the analysis of soluble ADAM9 protein levels in plasma samples. Data are presented as median (interquartile range) or mean ± SD.

* Non-smokers were all never-smokers. Smokers were defined as subjects that had ≥ 10 pack-year smoking history. Current smokers were defined as active smokers at the time of the sampling, or smoker who had stopped smoking ≤ 1 year before the sampling.

AJRCCM Articles in Press. Published on 04-June-2018 as 10.1164/rccm.201711-2300OC

[†]All COPD patients had forced expiratory volume in 1 second/ forced vital capacity ratio (FEV_1/FVC) < 0.7 whereas smokers without COPD and non-smoker controls had $FEV_1/FCV \geq 0.7$.

[‡]Categorical variables were analyzed with Chi-Square tests. Statistical analyses included One-Way ANOVA tests for continuous variables (age, FEV_1 % predicted, and FEV_1/FCV % predicted) followed by pair-wise comparisons using Student's t-tests or Mann-Whitney U tests.

[ll] The pack/year smoking histories of the GOLD stages I-II and GOLD stages III-IV COPD groups and the smoker group were significantly different from that of the non-smoker group by design ($P < 0.001$ for both comparisons). The pack/year smoking histories of the COPD GOLD stages I-II, and GOLD stages III-IV COPD groups were significantly different from that of the smoker group ($P = 0.008$ and $P < 0.001$, respectively).

[¶]The proportion of current smokers in the smoker and GOLD stage I-II, and GOLD stage III-IV COPD groups was significantly higher than that of the non-smoker group. However, the proportion of current smokers was similar in the smoker, and COPD GOLD stages I-II, and COPD GOLD stages III-IV groups.

[§]The FEV_1 of the GOLD stages III-IV COPD group was significantly lower than that of the smoker and non-smoker groups ($P < 0.001$ for both comparisons). The FEV_1 of the GOLD stages I-II COPD group was significantly lower than that of the smoker and non-smoker groups ($P < 0.001$ for both comparisons).

[§§]The FEV_1/FVC ratio of the GOLD stages III-IV COPD group was significantly lower than that of the smoker and non-smoker groups ($P < 0.001$ for both comparisons). The FEV_1/FVC ratio of

the GOLD stages I-II COPD group was also significantly lower than that of the smoker and non-smoker groups ($P < 0.001$ for both comparisons).

NS: Not significant.

AJRCCM Articles in Press. Published on 04-June-2018 as 10.1164/rccm.201711-2300OC

Table E3: Demographic and clinical characteristics of the subjects in the BALF and sputum cohort.

Characteristics of the BALF and sputum cohort	**Smokers* (N = 7)**	**COPD GOLD stages I-II (N = 20)**	**COPD GOLD stages III-IV (N = 8)**	***P* value‡**
Males (%)	3 (43)	17 (75)	6 (75)	***NS***
Age (yrs.)	52 ± 6	63 ± 6	66 ± 5	***P* < 0.001**
Pack-yrs. of smoking	26 (16-63)	41 (16-80)	47 (26-119)	***P* < 0.05**‖
Current smokers (%)	7 (100)	9 (45)	3 (38)	***P* < 0.**05¶
FEV_1 (% of predicted)	103 ± 11	62 ± 7	46 ± 5	***P* < 0.001**§
FEV_1/FVC (% of predicted)†	79 ± 4	50 ± 6	35 ± 6	***P* < 0.001**§§

The table shows the demographic and clinical characteristics of the COPD patients and smokers without COPD included for the analysis of soluble ADAM9 protein levels in sputum and BALF that were obtained from the same subjects (Manchester, UK cohorts). Data are presented as median (interquartile range) or mean ± SD.

*Smokers were defined as subjects that had ≥ 10 pack-year smoking history. Current smokers were defined as active smokers at the time of the sampling, or former smokers who had stopped smoking ≤ 1 year before the sampling.

[†]All COPD patients had forced expiratory volume in 1 second/ forced vital capacity ratio (FEV_1/FVC) < 0.7 whereas smokers without COPD and non-smoker controls had $FEV_1/FCV \geq 0.7$.

[‡]Categorical variables were analyzed with Chi-Square tests. Statistical analyses included one-way ANOVA tests for continuous variables (age, FEV_1 % predicted and FEV_1/FCV) followed by pair-wise comparisons using Student's t-tests or Mann-Whitney U tests.

[ll]The pack-year of smoking histories of the GOLD stages III-IV COPD group was significantly different from those of the smoker group ($P < 0.001$). The pack/year smoking histories of the GOLD stages I-II COPD group were also significantly different from those of the smoker group ($P < 0.05$).

[¶]The proportion of current smokers in the COPD GOLD stage I-II, and GOLD stage III-IV groups were significantly lower than that of the smoker group.

[§]The FEV_1 values of the GOLD stages III-IV COPD group and GOLD stages I-II COPD group were significantly different from those of the smoker group ($P < 0.001$ for both comparisons).

[§§]The FEV_1/FVC ratios of the GOLD stages III-IV COPD group and GOLD staged I-II COPD group were significantly different from those of the smoker group ($P < 0.001$ for both comparisons).

NS: not significant.

AJRCCM Articles in Press. Published on 04-June-2018 as 10.1164/rccm.201711-2300OC

Table E4: Demographic and clinical characteristics of the human bronchial epithelial cell (HBECs) donors.

Characteristics of the HBECs cohort	Controls* (N = 3)	COPD Patients* (N = 3)	*P* value
Males (%)	1 (33)	1 (33)	*NS*
Age (years)	65 ± 9	64 ± 12	*NS*
Pack-years smoking	N/A	42(5)	
Ever smoker (%)	2 (67)	3 (100) ‡	*NS*

The table shows the demographic and clinical characteristics of the COPD and control donors from whom the HBEC cells were obtained. The HBECs were used to measure surface staining for ADAM9, EGFR, VEGFR2, and assays to measure intracellular levels of phospho-Akt, total Akt, and active caspase-3. The HBECs were obtained from a commercial source, and limited demographic and clinical data were available from this source. Spirometry data were not available on any of the subjects studied.

Data are presented as number (percentage) or mean ± SD.

‡ Pack-year smoking histories were not available (N/A) for the control subjects.

NS: not significant.

Table E5: Demographic and clinical characteristics of subjects in the ADAM9, EGFR, and VEGFR2 immunostaining cohort.

Characteristics	Non-smokers* (N = 3)	Smokers* (N = 3)	COPD GOLD stages I-II (N = 3)	COPD GOLD stages III-IV (N = 3)	*P* value‡
Males (%)	1 (33)	2 (67)	3 (100)	1 (33)	***NS***
Age (years)	61 (44-77)	60 (53- 65)	64 (63- 65)	56 (55- 69)	***NS***‡
Pack-years of smoking	0 (0)	30 (25- 40)	30 (25- 80)	35 (30- 120)	***P* = 0.002**‖
Current smokers (%)	0	100	0	0	***NS***
FEV_1 (% of predicted)	102 ± 7	102 ± 11	59 ± 3	32 ± 9	***P* = 0.007**††
FEV_1/FVC (% of predicted)†	77 ± 5	78 ± 3	49 ± 6	44 ± 7	***P* < 0.05**§

The table shows the demographic and clinical characteristics of the COPD patients, smokers without COPD, and non-smokers in the Boston, USA lung immunostaining cohort (for analysis of ADAM9, EGFR, and VEGFR2 staining) who underwent a lung surgery or a lung biopsy.

* Non-smokers were all never-smokers. Smokers were defined as subjects that had $\geq$ 10 pack-year smoking history. Current smokers were defined as active smokers at the time of the surgery or lung biopsy, or former smokers who had stopped smoking $\leq$ 1 year before the surgery.

† All COPD patients had a forced expiratory volume in 1 second/ forced vital capacity (FEV_1/FVC) ratio < 0.7 whereas smokers without COPD and non-smoker controls had a FEV_1/FCV ratio $\geq$ 0.7.

AJRCCM Articles in Press. Published on 04-June-2018 as 10.1164/rccm.201711-2300OC

‡ Categorical variables were analyzed with Chi-Square tests. Continuous variables (FEV_1 % predicted and FEV_1/FCV) are presented as mean ± SEM and analyzed using One-Way ANOVAs followed by pair-wise comparisons using Student's t-tests. Non-continuous variables (age and pack-years) are presented as median (IQR) and analyzed using One-Way ANOVAs followed by pair-wise comparisons using Mann-Whitney tests.

ll The pack/year smoking histories of the smoker group was significantly higher than that of the non-smoker group (P = 0.002). The pack/year smoking histories of the GOLD stages III-IV and GOLD stages I-II COPD groups were not significantly different from that of the non-smoker group (P = 0.051 and P = 0.06, respectively). The pack/year smoking histories of the GOLD stages III-IV and GOLD stages I-II COPD groups were not significantly different from that of the smoker group (P = 0.4 and P = 0.5, respectively).

†† The FEV_1 % predicted values of the GOLD stages III-IV COPD group were significantly lower than those of the GOLD stages I-II COPD, smoker, and non-smoker groups (P = 0.04, 0.007, 0.01, respectively). The FEV_1 % predicted values of the GOLD stages I-II COPD group was significantly lower than those of the smoker and non-smoker groups (P = 0.02 and 0.008, respectively).

§ The FEV_1/FVC ratios of the GOLD stages III-IV and GOLD stages I-II COPD groups were significantly lower than those of the smoker and non-smoker groups by design ($P < 0.05$ for all comparisons).

NS: Not significant.

Table E6: Sequences of the primers used for Real-time PCR analysis of Adam9 gene expression in murine lung samples.

Gene	Forward primer	Reverse primer	Product Length (nucleotides)
Murine *Ppia*	GAGCTGTTTGCAGACAAAGTTC	CCCTGGCACATGAATCCTGG	125
Murine *β-Actin*	AGTGTGACGTTGACATCCGT	TGCTAGGAGCCAGAGCAGTA	120
Murine *Adam9*	GGAAGGCTCCCTACTCTCTGA	TCCAAAACTGGCATTCTCCAAA	148

The Table shows the sequences of the primers that were used to perform quantitative real-time RT-PCR to measure *Adam9* steady state mRNA levels in the lungs of WT mice exposed to air or smoke for 1 or 2 months or 6 months.

AJRCCM Articles in Press. Published on 04-June-2018 as 10.1164/rccm.201711-2300OC

Figure legends

Figure E1: Correlations between ADAM9 immunostaining in alveolar and bronchial epithelial cells and clinical parameters in the human lung immunostaining cohort: **A-B:** Correlations between ADAM9 immunostaining in alveolar epithelial cells (**A**) or bronchial epithelial cells (**B**) and pack-years of smoking history. **C-D:** Correlations between ADAM9 immunostaining in alveolar epithelial cells (**C**) or bronchial epithelial cells (**D**) and FEV_1/FVC. **E-F:** Scatter plots of ADAM9 immunostaining in alveolar epithelial cells (**E**) or bronchial epithelial cells (**F**) and percent predicted FEV_1. All data were analyzed using a linear regression model with ADAM9 staining parameters as the dependent variables, and the corresponding clinical parameters as the predictors. ADAM9 staining in alveolar epithelial cells was corrected for differences in age, current smoker status, and pack-year smoking histories between the groups. ADAM9 staining in bronchial epithelial cells was corrected for differences in the proportions of males between the groups; n = 31 subjects in each sub-figure including non-smokers, smokers, and COPD patients. $P < 0.05$ was considered to be statistically significant.

Figure E2: Correlations between ADAM9 staining in alveolar macrophages and clinical parameters in the human lung immunostaining cohort: **A-C** show correlations between ADAM9 immunostaining in alveolar macrophages and pack-year smoking history (**A)**; FEV_1/FVC (**B**); and FEV_1 percent predicted (**C**). All data were analyzed using the linear regression model with the ADAM9 staining parameter as the dependent variable, and the corresponding clinical parameters as the predictors. ADAM9 staining in alveolar macrophages was corrected for differences in the proportion of current smokers between the groups; n = 31 subjects including non-smokers, smokers, and COPD patients in all the figures. $P < 0.05$ was considered to be statistically significant.

Figure E3: Soluble ADAM9 (sADAM9) levels in BALF, plasma, and sputum samples from COPD patients, smokers, and non-smokers: **A**: Soluble ADAM9 (sADAM9) protein levels were measured in plasma samples from non-smokers (n = 28 subjects), smokers without COPD (n = 42 subjects), COPD GOLD stages I-II patients (n = 46 subjects) and COPD GOLD stages III-IV patients (n = 55 subjects) using an ELISA kit, and the results were log transformed (logarithm base 10 scale). The boxes in the box-plots show the medians and 25th and 75th percentiles, and the whiskers show the 10th and 90th percentiles. Data were analyzed using a Kruskal-Wallis One-Way ANOVA followed by pair-wise testing with Mann-Whitney U tests. **B**: sADAM9 protein levels were measured in BALF samples from smokers without COPD (n = 7 subjects), and COPD patients (n = 28 subjects) using an ELISA kit, and the results were log transformed (logarithm base 10 scale). The COPD patients were also sub-divided into COPD GOLD stages I-II patients (GOLD I-II, n = 20 subjects) and COPD GOLD stages III-IV patients (GOLD III-IV, n = 8 subjects). The boxes in the box-plots show the medians and 25th and 75th percentiles, and the whiskers show the 10th and 90th percentiles. Data were analyzed using a Bayesian linear regression adjusting for difference in age and pack-years of smoking history between the groups. **C**: sADAM9 protein levels were measured in spontaneously expectorated sputum samples from smokers without COPD (n = 7 subjects), and COPD patients (n = 28 subjects) using an ELISA kit, and the results were log transformed (logarithm base 10 scale). The COPD patients were also sub-divided into COPD GOLD stages I-II patients (GOLD I-II; n = 20 subjects) and COPD GOLD stages III-IV patients (GOLD III-IV; n = 8 subjects). The boxes in the box-plots show the medians and 25th and 75th percentiles, and the whiskers show the 10th and 90th percentiles. Data were analyzed using a Kruskal-Wallis One-Way ANOVA followed by pair-wise testing with Mann-Whitney U tests.

AJRCCM Articles in Press. Published on 04-June-2018 as 10.1164/rccm.201711-2300OC

Figure E4: Lung levels of cytokines and chemokines in CS-exposed WT and Adam9$^{-/-}$ mice. WT and *Adam9*$^{-/-}$ mice were exposed to air or CS for 1 month, and lung levels of Ccl-2 (**A**; n= 7-9 mice/group), Il-1β (**B**; n = 10 mice/group), G-csf (**C**; n = 8-12 mice/group), Il-10 (**D**; n = 10 mice/group), and active Tgf-β (**E**; n = 6-10 mice/group) were measured in homogenates of lung samples using commercial ELISA kits. Data were normalized to total protein levels measured in the same samples. The boxes in the box-plots show the medians and 25th and 75th percentiles, and the whiskers show the 10th and 90th percentiles. Data were analyzed using a Kruskal-Wallis One-Way ANOVA followed by pair-wise testing with Mann-Whitney U tests and Bonferroni corrections for multiple comparisons. *, $P < 0.025$ versus air-exposed mice belonging to the same genotype or the group indicated.

Figure E5: ADAM9 metalloproteinase domain does not cleave cytokines or chemokines that were elevated in the lungs of CS-exposed Adam9$^{-/-}$ mice. A: Active rhADAM9 (20 nM) versus assay buffer alone (as a control) were incubated with a quenched fluorogenic substrate that is susceptible to cleavage by ADAM9. Cleavage of the substrate was measured using fluorimetry. Data are mean + SD. The data shown are representative of 5 separate experiments. These experiments confirmed that the ADAM9 enzyme preparation was active. **B-D:** Recombinant human cytokines including 3200 nM CCL-5 (**B**), 2750 nM IL-8 (**C**), 900 nM IL-6 (**D**) and 1145 nM TNF-α (**E**) were incubated with or without 300 nM active rhADAM9 for 18 h with or without a non-selective metalloproteinase inhibitor (1-10 phenanthroline; 1, 10 phen) which inhibits ADAMs including ADAM9. Reaction products were separated on Tris-tricine gels and visualized with silver staining. Arrows indicate bands corresponding to ADAM9 and intact cytokines. **B-E** shows representative images of 4 separate experiments for each mediator. Note the lack of

degradation of each of the intact mediators and the lack of generation of lower molecular mass cleavage products of each of the mediators.

Figure E6: Adam9 does not regulate apoptosis of bone marrow-derived macrophages (BMDM) in vitro. BMDMs were isolated from unchallenged WT and *Adam9*$^{-/-}$ mice and exposed to 20% CSE for up to 48 h. Intracellular levels of active caspase-3 were measured using a quenched fluorogenic substrate, as described in Methods. Data are mean ± SD; n = 6 separate cell preparations. Data were analyzed using a One-Way ANOVA followed by pair-wise testing with Student's t-tests. There were no significant differences in intracellular active caspase-3 levels in WT or *Adam9*$^{-/-}$ cells at any time-point tested.

Figure E7: COPD patients have higher ADAM9 staining but lower EGFR and VEGFR2 staining in bronchial and alveolar epithelial cells than non-smoker and smoker controls: **A** and **B** show representative lung sections from non-smokers, smokers without COPD, and COPD patients (GOLD stages I-II and III-IV) that were triple immunostained with a red fluorophore (left panels) for a marker of airway epithelial cells (pan-cytokeratin; pan-CK in **A** and **B**), with a green fluorophore for ADAM9 (second panels in **A** and **B**) and with a cyanine fluorophore (white color) for EGFR or VEGFR2 (third panels in **A** and **B**, respectively). Nuclei in the lung sections were counter-stained blue using 4',6-diamidino-2-phenylindole (DAPI). The sections were examined using a confocal microscope. Merged images are shown in the right panels in **A** and **B** (magnification is x 400). Lung sections from a non-smoker were stained with a red fluorophore and non-immune murine (Ms) IgG, with a green fluorophore and non-immune goat (Goat) IgG, and with a cyanine fluorophore (white) and non-immune rabbit (Rb) IgG as controls (bottom panels). The images shown are representative of 3 subjects/group.

AJRCCM Articles in Press. Published on 04-June-2018 as 10.1164/rccm.201711-2300OC

References

1. Pierrou S, Broberg P, O'Donnell RA, Pawlowski K, Virtala R, Lindqvist E, Richter A, Wilson SJ, Angco G, Moller S, et al. Expression of Genes Involved in Oxidative Stress Responses in Airway Epithelial Cells of Smokers With Chronic Obstructive Pulmonary Disease. *Am J Respir Crit Care Med* 2007;175:577-586.

2. O'Donnell RA, Richter A, Ward J, Angco G, Mehta A, Rousseau K, Swallow DM, Holgate ST, Djukanovic R, Davies DE, et al. Expression of ErbB Receptors and Mucins in the Airways of Long Term Current Smokers. *Thorax* 2004;59:1032-1040.

3. Puddicombe SM, Polosa R, Richter A, Krishna MT, Howarth PH, Holgate ST, Davies DE. Involvement of the Epidermal Growth Factor Receptor in Epithelial Repair in Asthma. *FASEB J* 2000;14:1362-1374.

4. Laucho-Contreras ME, Taylor KL, Mahadeva R, Boukedes SS, Owen CA. Automated Measurement of Pulmonary Emphysema and Small Airway Remodeling in Cigarette Smoke-Exposed Mice. *J Vis Exp* 2015:52236. doi: 10.3791/52236.

5. Laucho-Contreras ME, Polverino F, Gupta K, Taylor KL, Kelly E, Pinto-Plata V, Divo M, Ashfaq N, Petersen H, Stripp B, et al. Protective Role for Club Cell Secretory Protein-16 (CC16) in the Development of Chronic Obstructive Pulmonary Disease. *Eur Respir J* 2015;45:1544-1556.

6. Roychaudhuri R, Hergrueter AH, Polverino F, Laucho-Contreras ME, Gupta K, Borregaard N, Owen CA. ADAM9 Is a Novel Product of Polymorphonuclear Neutrophils: Regulation

of Expression and Contributions to Extracellular Matrix Protein Degradation During Acute Lung Injury. *J Immunol* 2014;193:2469-2482.

7. Zhang D, Lee H, Cao Y, Dela Cruz CS, Jin Y. MiR-185 Mediates Lung Epithelial Cell Death After Oxidative Stress. *Am J Physiol Lung Cell Mol Physiol* 2016;310:L700-L710.

8. Knolle MD, Nakajima T, Hergrueter A, Gupta K, Polverino F, Craig VJ, Fyfe SE, Zahid M, Permaul P, Cernadas M, et al. Adam8 Limits the Development of Allergic Airway Inflammation in Mice. *J Immunol* 2013;190:6434-6449.

9. Lee H, Zhang D, Zhu Z, Dela Cruz CS, Jin Y. Epithelial Cell-Derived Microvesicles Activate Macrophages and Promote Inflammation Via Microvesicle-Containing MicroRNAs. *Sci Rep* 2016;6:35250.

10. Owen CA, Campbell MA, Sannes PL, Boukedes SS, Campbell EJ. Cell-Surface-Bound Elastase and Cathepsin G on Human Neutrophils. A Novel, Non-Oxidative Mechanism by Which Neutrophils Focus and Preserve Catalytic Activity of Serine Proteinases. *J Cell Biol* 1995;131:775-789.

11. Zhang D, Wang X, Li Y, Zhao L, Lu M, Yao X, Xia H, Wang YC, Liu MF, Jiang J, et al. Thyroid Hormone Regulates Muscle Fiber Type Conversion Via MiR-133a1. *J Cell Biol* 2014;207:753-766.

AJRCCM Articles in Press. Published on 04-June-2018 as 10.1164/rccm.201711-2300OC

Figure E1

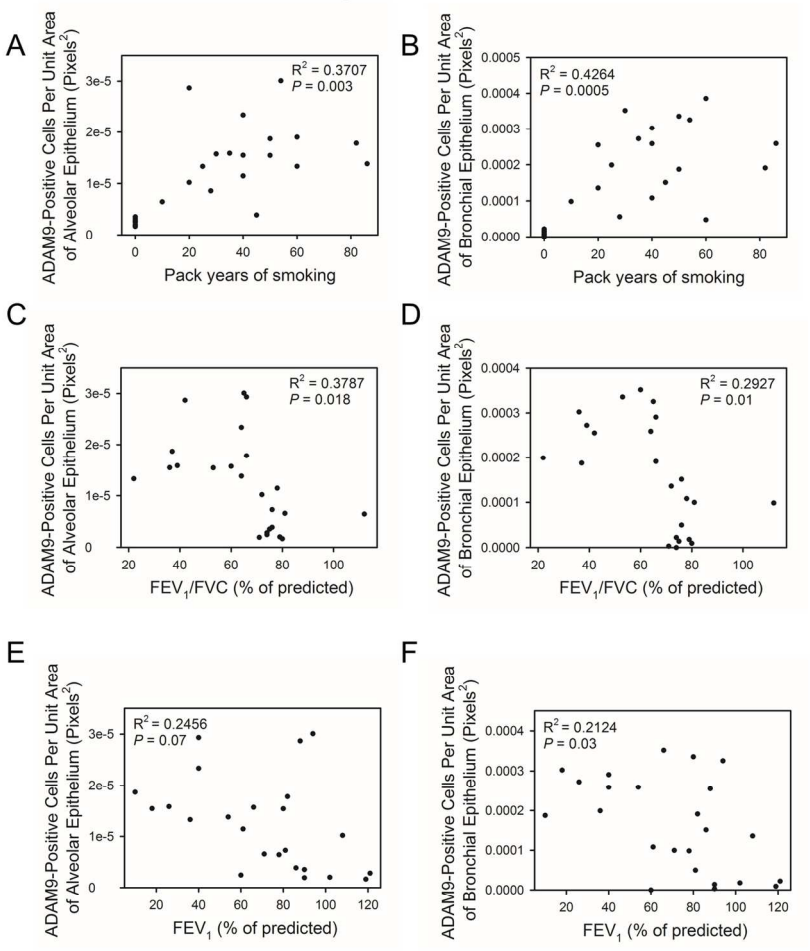

130x173mm (300 x 300 DPI)

Figure E2

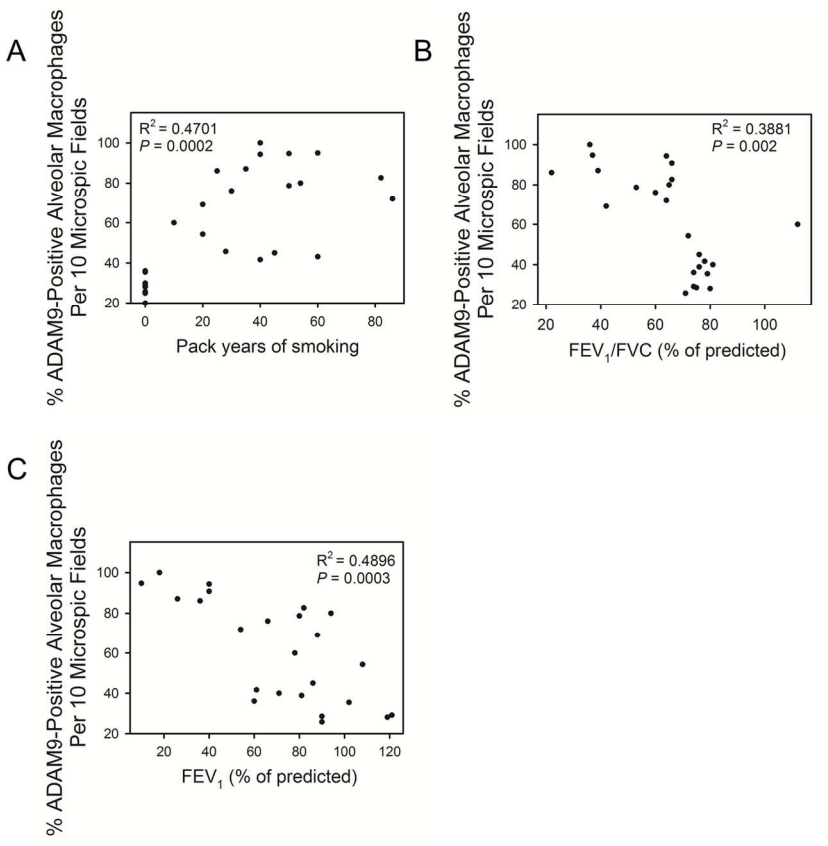

130x173mm (300 x 300 DPI)

AJRCCM Articles in Press. Published on 04-June-2018 as 10.1164/rccm.201711-2300OC

Figure E3

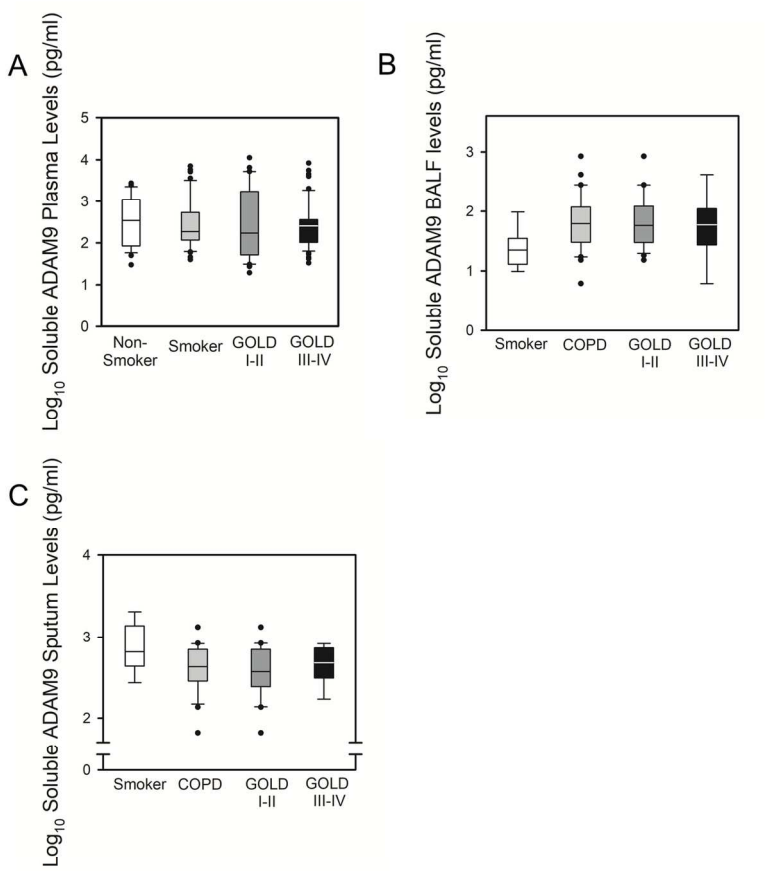

130x173mm (300 x 300 DPI)

Figure E4

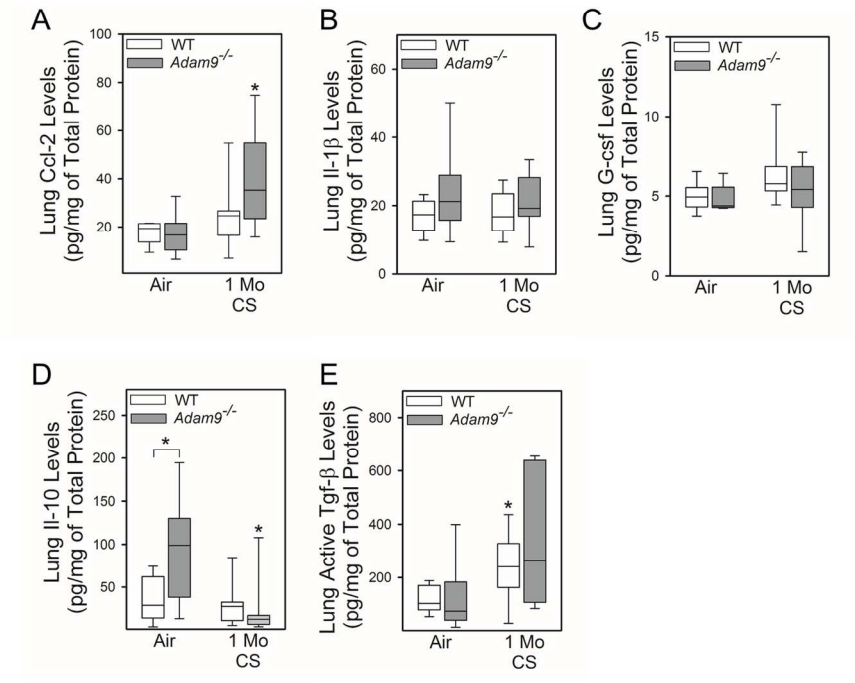

130x173mm (300 x 300 DPI)

AJRCCM Articles in Press. Published on 04-June-2018 as 10.1164/rccm.201711-2300OC

Figure E5

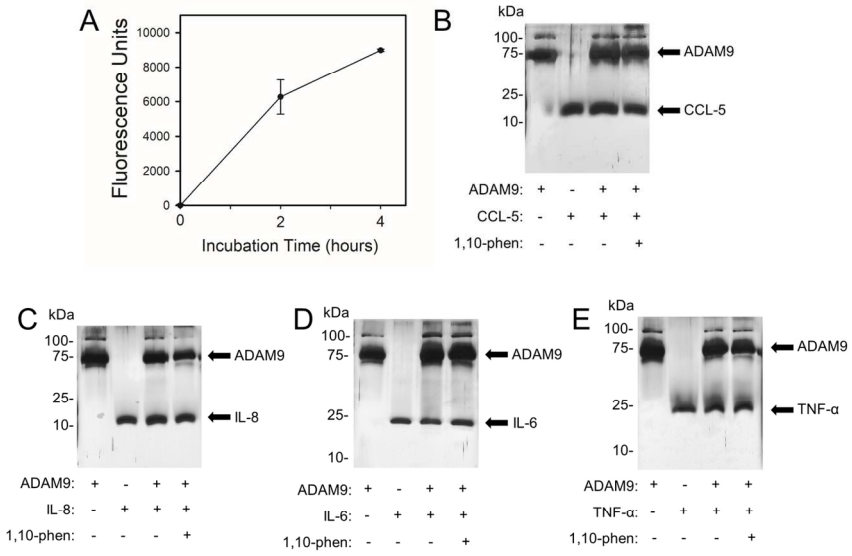

130x173mm (300 x 300 DPI)

Figure E6

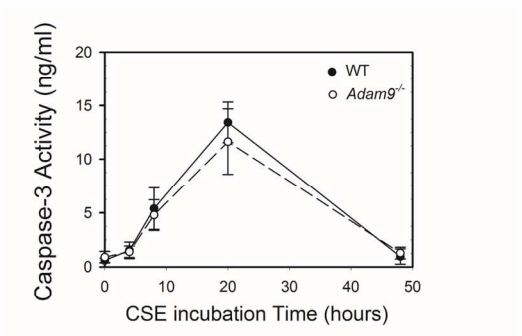

130x173mm (300 x 300 DPI)

AJRCCM Articles in Press. Published on 04-June-2018 as 10.1164/rccm.201711-2300OC

Figure E7

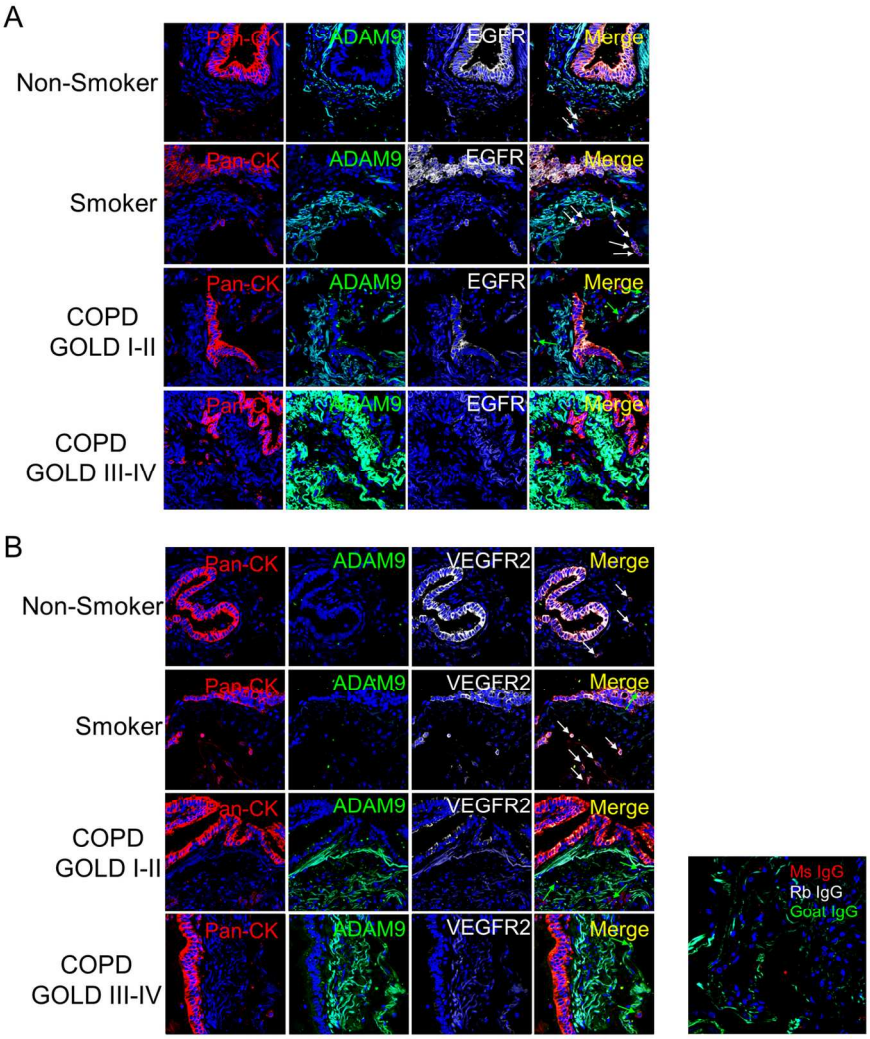

130x173mm (300 x 300 DPI)